

**Dear editor,**

**we are very thankful the referees for helpful and constructive comments and recommendations. We have revised the paper in accordance with the reviewers' suggestions to produce an improved version of our manuscript.**

**Answers to reviewer comments.**

**Reviewer 1**

**Comment:** *However, before it can be published in Biogeosciences, the authors need to take the major concern into account that I highlighted in the online discussion. It is my concern that this study has several limitations due to the fact that the results are based on only a single fluxtower site, while analysing the impact of a large scale phenomenon (ENSO). In their response letter the authors agree with this comment. But in the manuscript this limitation is not discussed.*

*I fully understand that the authors are now not able to include additional fluxtowers for this data poor region. But the authors should include at least an additional paragraph in the discussion section that discusses thoroughly the limitations of using only 1 site for this type study. Is the site representative for the region? Is the site affected by local climate phenomena that interact with the ENSO responses? ... Maybe refer to other studies where multiple fluxtowers in the same region responded similar/differently to large scale climate patterns...*

**Answer:**

Yes, we agree with reviewer, that the limitations of the “one-site study” should be mentioned and discussed. We added following text in the Discussion section:

“Even though remote sensing analyses have shown that the site is representative for the region (Ibrom et al. 2007, Popastin et al. 2012), the response to ENSO might differ in the region dues to differences in altitude and land-use (Erasmi et al. 2009). In general, anthropogenic deforestation has removed most parts of lowland forests so that the remaining forest cover consists mostly of mountainous forests. At the moment, there are no other FLUXNET sites situated in equatorial mountainous rainforests of South-East Asia with which we could directly compare our findings and investigate whether similar response to ENSO can be observed. Most of the existing FLUXNET sites (AsiaFlux) are not comparable with the investigated site as they are situated in subequatorial and tropical climate zones. These are characterized by higher seasonality of air temperature and precipitation compared to our equatorial site. Thus, our site provides a unique opportunity to investigative the response of an equatorial mountainous rainforest to ENSO in the Western pacific region”

**Comment:** *In a similar way, the authors should acknowledge the limitations of using an open-path sensor.*

**Answer.**

We used an open-path sensor due to the low power availability at the site (only solar power). In the manuscript we now extended the explanation how we circumvented the usual consequences of open-path sensor measurements by using a process model for gap-filling. (see page 6 of the manuscript, line 8 to 33) :

“For filling the gaps in the measured Net Ecosystem Exchange (NEE) and evapotranspiration, net radiation, sensible and latent heat flux records as well as to quantify GPP, RE and forest canopy transpiration the process-based Mixfor-SVAT model (Olchev et al., 2002; 2008) was used.

Mixfor-SVAT is a one-dimensional model of the energy, H<sub>2</sub>O and CO<sub>2</sub> exchange between vertically structured mono- or multi-specific forest stands and the atmosphere. The main model advantage is its ability both to describe seasonal and daily patterns of CO<sub>2</sub> and H<sub>2</sub>O fluxes at

individual tree and entire ecosystem levels and to estimate the contributions of soil, different forest layers, and various tree species into the total ecosystem fluxes taking into account individual structure, biophysical properties and responses of plant species to changes in environmental conditions. The model also allows to take into account the non-steady-state water transport in the trees, rainfall interception, dew generation, turbulence and convection flows within the canopy and plant canopy energy storage. As model input the measured meteorological variables (air temperature, water vapor pressure, wind speed, precipitation, CO<sub>2</sub> concentration, global solar radiation) are used. The model was tested with long-term meteorological and flux data from different experimental sites including the investigated forest under well-developed turbulent conditions and showed a good agreement over a broad spectrum of weather and soil moisture conditions (Olchev et al., 2002; Falk et al., 2005; Falge et al., 2005; Olchev et al., 2008). Using the model is superior to common statistical gap-filling approaches, because these depend on calibration under all relevant weather conditions, including those that were systematically excluded when the open-path sensor did not work, e.g. under rain. For this reason one might argue that statistical gap-filling is biased by calibration during dry weather conditions. The process-based model is, however, able to take these weather situations into account, because it is based on general physical principles. As it was shown in previous studies the model is able to predict both CO<sub>2</sub> and water fluxes under various weather and soil moisture conditions at sites where closed-path sensors were used (Olchev et al., 1996; Falge et al., 2005)."

## Reviewer 2

**Comment:** Although I acknowledge the fact that the authors now explicitly limit their conclusions to monthly anomalies, their answer to my question about the absolute magnitude of NEE (as shown in Fig. 2) is insufficient. In their response letter, the authors compare GPP with that of other tropical forests (with which it agrees) and argue that RE must be lower than in those other forests due to the lower temperatures prevailing in the mountains and, as a consequence, NEE must be very large. Well, a continuous net uptake at a record-high average rate of nearly 1 kg C m<sup>-2</sup>a<sup>-1</sup> must correspond to a steady and sustainable carbon accumulation in either wood or litter or soil (or in several components). How could this be possible and where do the authors think that the carbon goes? Can they provide any independent validation, e.g. through measurements of wood or biomass increment or soil carbon stock? This I would consider as a pre-requisite for defending the NEE rates shown in the ms. If there are no such data available yet, the authors may consider asking foresters for advice on how to conduct such measurements at a remote site without too much effort. The reason why I am insisting on this point is that the results shown in Fig. 2 would have a huge impact if it really was true that old-growth forests are such extremely strong carbon sinks.

### Answer.

We thank for the advice to track the carbon in the system. This additional data will certainly lead to an interesting new study on the carbon budget of the site. However it will hardly be possible to achieve the requested accuracy in a short time period and still the uncertainty of below ground carbon allocation will remain. The focus of this study is not the carbon budget, but its sensitivity on seasonal weather anomalies. We discuss deviations from the mean and not the carbon budget.

In our first revisions we have corroborated our values with additional analyses on daytime NEE, which is independent from nighttime low turbulence phenomena. These analyses have shown that the findings using whole day NEE were robust.

On the other hand we do not see why we should not mention the measured budget. Annual estimations of NEE of CO<sub>2</sub> for our tropical forest is 7.29±0.32 t C ha<sup>-1</sup> (not 10 t C ha<sup>-1</sup>). As it was already mentioned our GPP, Re and NEE values are reasonably close to the average values for tropical forests as it was reported in Luyssaert et al. (Global Change Biology, 2007, 13, 2509–2537), 75–538 g C m<sup>-2</sup> yr<sup>-1</sup>. In present time in the literature it can be found a much larger estimations of the net CO<sub>2</sub> uptake rates for old but at the same time rapidly growing tropical forests (e.g. of the annual NEE in the mangrove forests of Everglades National Park (Florida, USA) showed that the NEE can reach 1200 g m<sup>-2</sup> yr<sup>-1</sup> (Barr, J. G., Engel, V.C., Fuentes, J.D., Zieman, J.C., O'Halloran, T.L., Smith III, T.J., Anderson, G.H., 2010. Controls on mangrove forest-atmosphere carbon dioxide exchanges in western Everglades National Park. J. Geophys. Res. Biogeosci.).

In the manuscript, we have briefly discussed that these numbers are high, and which potential reason there are for this, e.g. site history and regrowth after selected use of large individual trees by the local population (chapter 4.1, page 11-12).

**Comment:** Filtering with  $ustar > 0.25 \text{ m/s}$  does not remove the doubts about the soil CO<sub>2</sub> efflux data, either, since it is not clear, given the nevertheless sloping terrain and the maximum tree height of 36 m, whether any eddies at all penetrate to the ground. It is still possible that the CO<sub>2</sub> efflux from the soil remains always decoupled from the eddy flux above the canopy, with most of the soil CO<sub>2</sub> flowing down the slope. Are there any CO<sub>2</sub> chamber measurements of soil respiration that could be shown for comparison or any turbulence data from within the canopy? Alternatively, are there any other studies that show such data in tall tropical forests and that could be cited?

### Answer.

If we understand the reviewer correctly she or he wants to consider the theoretical possibility that all or a constant fraction of the CO<sub>2</sub> transport from the soil is entirely decoupled from the air layer

above the forest. We show that the nighttime fluxes increase with  $u^*$  and that they level off beyond a certain  $u^*$  threshold value. This would imply a flux loss component that is  $u^*$  dependent and a component that is independent from  $u^*$ . We don't know of any published empirical findings or theoretical analyses that back such an assumption. On the contrary it has been shown that at some sites the night time fluxes increase over the whole range of  $u^*$ , i.e. no  $u^*$  threshold could be found (Fig. 3 in Loescher, H., Oberbauer, S.H., Gholz, H.L. and Clark, D.A., 2003. Environmental control on net ecosystem-level carbon exchange and productivity in a Central American tropical wet forest. *Global Change Biology*, 9: 396-412.). In such sites, the problem limited mixing is permanent, we have shown that this is not the case at our site.

To minimise a potential bias on the flux sums, we used a process-based forest model that is not biased by a lack of data in wet and low turbulence conditions. Model estimations (calibrated using the chamber data) of annual soil respiration for Bariri site is about  $11.1 \pm 0.3 \text{ t C ha}^{-1} \text{ yr}^{-1}$ . This value is close to averaged estimates of the soil  $\text{CO}_2$  efflux obtained by van Straaten et al. (2011) for the central Sulawesi region ( $11.7 \text{ t C ha}^{-1} \text{ yr}^{-1}$ ).

**Comment:** *Alternatively, are there any other studies that show such data in tall tropical forests and that could be cited.*

See the first answer to Reviewer 2

Also we refer in our study to Luyssaert et al. (*Global Change Biology*, 2007, 13, 2509–2537)

**Comment:** *Last, but not least, I am irritated by the fact that the authors, in some places, did in fact not change the manuscript text according to what they announced in the response letter. Examples: "In our revised manuscript, we will describe the gap-filling approach and the model in more detail." They did not.*

**Answer:**

We are sorry for any irritation the response might have caused.

In page 6 we indicated that for the gap filling in the time series of  $\text{CO}_2$  fluxes, as well as for the gaps in net radiation, sensible and latent heat flux records the process-based Mixfor-SVAT model (Olchev et al., 2002; 2008) was applied. The general description of the model is given in many previous publication e.g. Olchev et al., 2002; 2008 , Falk et al., 2005; Falge et al., 2005. We included the references in the manuscript. According to the reviewers' suggestion a more detailed description of the gap filling procedure is provided on page 6:

"For filling the gaps in the measured Net Ecosystem Exchange (NEE) and evapotranspiration, net radiation, sensible and latent heat flux records as well as to quantify GPP, RE and forest canopy transpiration the process-based Mixfor-SVAT model (Olchev et al., 2002; 2008) was used.

Mixfor-SVAT is a one-dimensional model of the energy,  $\text{H}_2\text{O}$  and  $\text{CO}_2$  exchange between vertically structured mono- or multi-specific forest stands and the atmosphere. The main model advantage is its ability both to describe seasonal and daily patterns of  $\text{CO}_2$  and  $\text{H}_2\text{O}$  fluxes at individual tree and entire ecosystem levels and to estimate the contributions of soil, different forest layers, and various tree species into the total ecosystem fluxes taking into account individual structure, biophysical properties and responses of plant species to changes in environmental conditions. The model also allows to take into account the non-steady-state water transport in the trees, rainfall interception, dew generation, turbulence and convection flows within the canopy and plant canopy energy storage. As model input the measured meteorological variables (air temperature, water vapor pressure, wind speed, precipitation,  $\text{CO}_2$  concentration, global solar radiation) are used. The model was tested with long-term meteorological and flux data from different experimental sites including the investigated forest under well-developed turbulent conditions and showed a good agreement over a broad spectrum of weather and soil moisture conditions (Olchev et al., 2002; Falk et al., 2005; Falge et al., 2005; Olchev et al., 2008). Using the model is superior to common statistical gap-filling approaches, because these depend on calibration under all relevant weather conditions, including those that were systematically excluded when the open-path sensor did not work, e.g.

under rain. For this reason one might argue that statistical gap-filling is biased by calibration during dry weather conditions. The process-based model is, however, able to take these weather situations into account, because it is based on general physical principles. As it was shown in previous studies the model is able to predict both CO<sub>2</sub> and water fluxes under various weather and soil moisture conditions at sites where closed-path sensors were used (Olchev et al., 1996; Falge et al., 2005)."

**Comment:** *The respective text (last 9 lines of section 2.3) was left completely unchanged. (Only the preceding sentences about the ustar filtering were added.) "The discussion about data uncertainty will be added to the revised version of the manuscript." It wasn't! No error margins at all are presented in the text, just a few standard deviations for some multi-year records. Whether this was simply forgotten or deliberately omitted I cannot judge, but in any case the authors should keep the promises they made in their response letter.*

**Answer:**

The explanation was added in the first part of discussion (chapter 4.1 " Uncertainty of the analysis ", page 11-12):

"Eddy covariance flux measurements in tropical mountainous conditions are challenging. Our tower and eddy covariance system was designed to minimise power consumption by using an open-path sensor, which had the consequence that rainy conditions systematically caused gaps in the flux data. To minimise a potential bias on the flux sums, we used a process-based forest model that is not biased by a lack of data in wet conditions as the often used statistical gap-filling algorithms (Reichstein et al., 2005, see also section 2.3). The weather in the tropics typically has a relatively high percentage of calm nights. The selected forest is located on a plateau in a mountainous region and this increases the risk of CO<sub>2</sub> rich air draining downhill in calm night. We investigated this effect very carefully and found that the CO<sub>2</sub> fluxes showed a very clear  $u_*$  threshold above which the night time CO<sub>2</sub> emission rates did not depend on  $u_*$  anymore. Using only data from nights with sufficient turbulence ( $u_* > u_*$  threshold value) we minimised advection and drainage affecting the NEE estimates. Also, here we benefitted from the use of the process model for gap-filling.

In addition we compared the model predicted mean annual soil respiration rate with soil CO<sub>2</sub> efflux data that were measured in the study region with soil chambers (van Straaten et al. 2011). The Mixfor-SVAT model estimated an average annual soil respiration rate of  $1110 \pm 30$  g C m<sup>-2</sup> yr<sup>-1</sup> for the investigated site. This value was very close to the measured average soil CO<sub>2</sub> efflux of for the central Sulawesi region of  $1170$  g C m<sup>-2</sup> yr<sup>-1</sup> which shows realistic behavior of the model.

We then analysed the statistical relationships between our gap-filled monthly fluxes with climate anomaly indices and corroborated these analyses also with midday NEE data only. As time data are independent from night time data, we made sure that our analysis was not affected by night time flux loss. The correlations with midday data and ENSO indices were very similar to those with daily mean NEE data. This demonstrated the robustness of our analysis.

The relatively high annual NEE sums need further investigation. After applying all corrections including the correction for open-path sensor heating, and after gap filling we found an average annual uptake of  $729 \pm 32$  g C m<sup>-2</sup> yr<sup>-1</sup> (standard deviation between 5 different years). This value is higher as the range found in lowland rain forests, i.e. ranging from e.g. 75 to 538 g C m<sup>-2</sup> yr<sup>-1</sup> (Luyssaert et al., 2007). The clarification of this very interesting phenomenon, maybe relating to the site history and regrowth after selected use of large individual trees by the local population, lies however not within the scope of this article.

1   **Response of CO<sub>2</sub> and H<sub>2</sub>O fluxes of a mountainous tropical**  
2   **rainforest in equatorial Indonesia to El Niño events**

3  
4   **A. Olchev<sup>1,2</sup>, A. Ibrom<sup>3</sup>, O. Panferov<sup>4</sup>, D. Gushchina<sup>5</sup>, H. Kreilein<sup>2</sup>, V. Popov<sup>6,7</sup>, P.**  
5   **Propastin<sup>2</sup>, T. June<sup>8</sup>, A. Rauf<sup>9</sup>, G. Gravenhorst<sup>\*</sup> and A. Knohl<sup>2</sup>**

6  
7   [1] {A.N. Severtsov Institute of Ecology and Evolution of RAS, Moscow, Russia}

8   [2] {Department of Bioclimatology, Faculty of Forest Sciences and Forest Ecology, Georg-August  
9   University of Goettingen, Goettingen, Germany}

10   [3] {Centre for Ecosystems and Environmental Sustainability, Department of Chemical and  
11   Biochemical EngineeringDepartment for Environmental Engineering, Technical University of  
12   Denmark, RoskildeKgs. Lyngby, Denmark}

13   [4] {Climatology and Climate Protection, Faculty of Life Sciences and Engineering, University of  
14   Applied Sciences, Bingen am Rhein, Germany}

15   [5] {Department of Meteorology and Climatology, Faculty of Geography, Moscow State  
16   University, Moscow, Russia}

17   [6] {Faculty of Physics, Lomonosov Moscow State University, Moscow, Russia}

18   [7] {Financial University under the Government of the Russian Federation, Moscow, Russia}

19   [8] {Bogor Agricultural University, Department of Geophysics and Meteorology}

20   [9] {Universitas Tadulako, Palu, Indonesia}

21   [\*] {Retired}

22  
23   Correspondence to: A. Olchev (aoltche@gmail.com)

24

25   **Abstract**

26         The possible impact of El Niño-Southern Oscillation (ENSO) events on the main  
27         components of CO<sub>2</sub> and H<sub>2</sub>O fluxes between tropical rainforest and atmosphere is investigated. The  
28         fluxes were continuously measured in a old-growthpristine mountainous tropical rainforest growing  
29         in Central Sulawesi in Indonesia using the eddy covariance method for the period from January  
30         2004 to June 2008. During this period, two episodes of El Niño and one episode of La Niña were  
31         observed. All these ENSO episodes had moderate intensity and were of Central Pacific type. The  
32         temporal variability analysis of the main meteorological parameters and components of CO<sub>2</sub> and  
33         H<sub>2</sub>O exchange showed a high sensitivity of Evapotranspiration (ET) and Gross Primary Production  
34         (GPP) of the tropical rainforest to meteorological variations caused by both El Niño and La Niña

1 episodes. Incoming solar radiation is the main governing factor that is responsible for ET and GPP  
2 variability. Ecosystem Respiration (RE) dynamics depend mainly on the air temperature changes  
3 and are almost insensitive to ENSO. Changes of precipitation due to moderate ENSO events did not  
4 cause any notable effect on ET and GPP, mainly because of sufficient soil moisture conditions even  
5 in periods of anomalous reduction of precipitation in the region.

6

## 7 **1. Introduction**

8 The contribution of tropical rainforests to the global budget of greenhouse gases, their  
9 possible impact on the climatic system, and their sensitivity to climatic changes are key topics of  
10 numerous theoretical and experimental studies (Clark and Clark, 1994; Grace et al., 1995, 1996;  
11 Malhi et al., 1999; Ciais et al., 2009; Lewis et al., 2009; Phillips et al., 2009; Malhi, 2010; Fisher et  
12 al., 2013; Moser et al., 2014). The area covered by tropical rainforests was drastically reduced  
13 during the last century, mainly due to human activities and presently there are less than 11.0 million  
14 km<sup>2</sup> remaining (Malhi, 2010). While deforestation rates in the tropical forests of Brazil are now  
15 declining, countries in South-East Asia, particularly Indonesia, show globally the largest increase in  
16 forest loss (Hansen et al., 2013), resulting in major changes in carbon and water fluxes between the  
17 land surface and the atmosphere. Therefore, during the last decade the tropical forest ecosystems of  
18 South-East Asia and especially Indonesia are the focus area of intensive studies of biogeochemical  
19 cycle and land surface - atmosphere interactions. On the one hand, it is necessary to know how  
20 these tropical forests influence the global and regional climate, and on the other hand, how they  
21 respond to changes of regional climatic conditions.

22 Climate and weather conditions in the equatorial Pacific and South-Eastern part of Asia are  
23 mainly influenced by the Intertropical Convergence Zone (ITCZ) which is seasonally positioned  
24 north and south of the equator. Another very important factor affecting the climate of South-East  
25 Asia is the well-known coupled oceanic and atmospheric phenomenon, El Niño-Southern  
26 Oscillation (ENSO). During the warm phase of ENSO, termed "El Niño", sea surface temperature  
27 (SST) in the central and eastern parts of the equatorial Pacific sharply increases, and during a cold  
28 phase of the phenomenon, termed "La Niña", the SST in these areas is lower than usual. Both  
29 phenomena, El Niño and La Niña, lead to essential changes of pressure distribution and atmospheric  
30 circulation and, as a result, to anomalous changes of precipitation amount, solar radiation, and  
31 temperature fields, both in the regions of sea surface temperature anomalies and in a wide range of  
32 remote areas through the mechanism of atmospheric bridges (Wang, 2002; Graf and Zanchettin,  
33 | 2012; Yuan and Yan, 2013). Typically, in Indonesia El Niño results in dryer conditions and La Niña  
34 results in wetter conditions, potentially impacting the land vegetation (Erasmi et al., 2009). ENSO

1 events are irregular, characterised by different intensity and, are usually observed at intervals of 2-7  
2 years.

3 To describe the possible effects of ENSO events on CO<sub>2</sub> and H<sub>2</sub>O exchange between land  
4 surface and the atmosphere, many studies for different Western Pacific regions were carried out  
5 during the recent decades (Feely et al., 1998; Malhi et al., 1999; Rayner and Law, 1999; Aiba and  
6 Kitayama, 2002; Hirano et al., 2007; Erasmi et al., 2008; Gerold and Leemhuis, 2010). They are  
7 mainly based on the results of modelling experiments and remote sensing data (Rayner and Law,  
8 1999). Experimental results based on direct measurements of CO<sub>2</sub> and H<sub>2</sub>O fluxes, which allow  
9 studying the response of individual terrestrial ecosystems to anomalous weather conditions, are still  
10 very limited (e.g. Hirano et al., 2007; Moser et al., 2014). Existing monitoring networks in  
11 equatorial regions of the Western Pacific are associated mainly with lowland areas and do not cover  
12 mountainous rainforest regions, even though mountainous regions cover some of the last remaining  
13 undisturbed rainforest in South-East Asia. Most attention in former studies was paid to the  
14 description of plant response to anomalously dry and warm weather during El Niño events (Aiba  
15 and Kitayama, 2002; Hirano et al., 2007; Moser et al., 2014). The possible changes in plant  
16 functioning during La Niña events are still not clarified. In particular, Malhi et al. (1999) reported  
17 that for Amazon region in the South America El Niño periods are strongly associated with enhanced  
18 dry seasons that probably result in increased carbon loss, either through water stress causing  
19 reduced photosynthesis or increased tree mortality. Aiba and Kitayama (2002) examined the effects  
20 of the 1997–98 El Niño drought on nine rainforests of Mount Kinabalu in Borneo using forest  
21 inventory and showed that El Niño increased the tree mortality for lowland forests. However, it did  
22 not affect the growth rate of the trees of upland forests (higher than 1,700 m) where mortality was  
23 restricted by some understorey species only. Eddy covariance measurements of the CO<sub>2</sub> fluxes in a  
24 tropical peat swamp forest in Central Kalimantan, Indonesia, for the period from 2002 to 2004,  
25 provided by Hirano et al. (2007), showed that during the El Niño event in the period November–  
26 December 2002 the annual net CO<sub>2</sub> release reached maximal values, mainly due to strong decrease  
27 of GPP in the late dry season, because of dense smoke emitted from large-scale fires. Effects of El  
28 Niño on annual RE in 2002 were insignificant.

29 There is a lack of experimental data on CO<sub>2</sub> and H<sub>2</sub>O fluxes in mountainous rainforests in  
30 equatorial regions of the Western Pacific, and on their response to ENSO. Hence, the main  
31 objective of this study was to evaluate and quantify the impact of ENSO events on the main  
32 components of CO<sub>2</sub> and H<sub>2</sub>O fluxes in an old-growthpristine mountainous tropical rainforest  
33 growing in Central Sulawesi, Indonesia. The methodology used was analysis of long-term eddy  
34 covariance flux measurement data.

1    **2. Materials and Methods**

2    **2.1 El Niño's types and intensity**

3         Nowadays, two types of ENSO can be distinguished: 1) the canonical or conventional El  
4         Niño, which is characterised by SST anomalies located in the eastern Pacific near the South  
5         American coast (Rasmusson and Carpenter, 1982) and 2) the Central Pacific El Niño or El Niño  
6         Modoki (Larkin and Harrison, 2005; Ashok et al., 2007; Kug et al., 2009; Ashok and Yamagata,  
7         2009; Gushchina and Dewitte, 2012). In 2003, ~~a the~~ new definition of the conventional El Niño was  
8         accepted by the National Oceanic and Atmospheric Administration (NOAA) of the USA, in  
9         referring to the warming of the Pacific region between 5°N - 5°S and 170° - 120°W. According to  
10      Ashok et al. (2007) the Central Pacific El Niño/El Niño Modoki - i.e. unusually high SST - occurs  
11      roughly in the region between 160°E - 140°W and 10°N - 10°S.

12         As criteria to assess the intensity of ENSO events, a wide range of indexes based on  
13      different combinations of sea level pressure and SST data in various areas of the Pacific are used.  
14      For diagnostics of the central Pacific El Niño, the SST anomalies (in °C) in Nino4 region (5°N -  
15      5°S and 160°E - 150°W) are broadly used (Figure 1). The monthly SST anomalies (in °C) in  
16      Nino3.4 region (5°N - 5°S and 170° - 120°W) are used to diagnose both types of El Niño  
17      phenomenon: canonical and Central Pacific (Download Climate Timeseries, 2013).

18

19    **2.2 Experimental site**

20         The tropical rainforest selected for the study is situated near the village Bariri in the southern  
21      part of the Lore Lindu National Park of Central Sulawesi in Indonesia (1°39.47'S and 120°10.409'E  
22      or UTM 51S 185482 m east and 9816523 m north) (Figure 1). The site is located on a large plateau  
23      of several kilometres in size at about 1,430 m above sea level surrounded by mountain chains  
24      surmounting the plane by another 300 m to 400 m. Within 500 m around the tower the elevation  
25      varies between 1,390 and 1,430 metres. Wind field measurement with a sonic anemometer indicate  
26      a slope of around 2-3°, which is similar to many Fluxnet sites. About 1,000 m to the east from the  
27      experimental site, the forest is replaced by a meadow; in all other directions the forest extends  
28      several kilometres ~~-(~~Ibrom et al., 2007).

29         According to the Köppen climate classification the study area relates to tropical rainforest  
30      climate (*Af*) (Chen-D. and Chen-H.W., 2013). Weather conditions of the region are mainly  
31      influenced by the ITCZ. During the wet season (typically, from November to April) the area is  
32      influenced by very moist northeast monsoons coming from the Pacific. Maximum precipitation  
33      during the observation period from January 2004 to July 2008 was observed in April - with  
34       $258.0 \pm 148.0 \text{ mm month}^{-1}$ . The drier season usually lasts from May to October. The precipitation

minimum was observed in September with  $195.0 \pm 48.0$  mm month $^{-1}$ . The September-October period was also characterised by maximal incoming solar radiation, up to  $650 \pm 47.0$  MJ m $^{-2}$  month $^{-1}$ , mainly because of a significant decrease of convective clouds, due to the reversing of oceanic northeast monsoon to a southeast monsoon blowing from the Australian continent. The mean annual precipitation amount exceeded 2000 mm. The mean monthly air temperature varies between 19.4 °C and 19.7 °C. The mean annual air temperature was 19.5 °C (Falk et al., 2005; Ibrom et al., 2007).

The vegetation at the experimental site is very diverse and ~~very representative to-for the mountainous montane tropical rainforest communities of the Central Sulawesi. It is represented by~~ There are about more than 88 different tree species per hectare. Among the dominant species are *Castanopsis accuminatissima* BL. (29%), *Canarium vulgare* Leenh. (18%) and *Ficus spec.* (9.5%). The density of trees, with diameter at breast height larger than 0.1 m, is 550 trees per ha. In addition, there is more than a 10-fold larger number of smaller trees per hectare with stem diameter lower than 0.1 m. The total basal area of trees reached 53 m $^2$  per ha. Leaf area index (LAI) is about 7.2 m $^2$  m $^{-2}$ . LAI has been estimated using an indirect hemispherical photography approach with a correction for leaf clumping effects. The height of the trees, with diameters at breast height larger than 0.1 m, varies between the lowest at 12 m and the highest at 36 m. The mean tree height is 21 m (Ibrom et al., 2007).

### 2.3 Flux measurements and gap filling

CO<sub>2</sub> and H<sub>2</sub>O fluxes were measured from 2004 to 2008 within the framework of the STORMA project (Stability of Rainforest Margins in Indonesia, SFB 552), supported by the German Research Foundation (DFG). Eddy covariance equipment for flux measurements was installed on a meteorological tower of 70 m height at the 48 m level, i.e. ca. 12 m higher than the maximal tree height. The measuring system consists of a three-dimensional sonic anemometer (USA-1, Metek, Germany) and an open-path CO<sub>2</sub> and H<sub>2</sub>O infrared gas analyzer (IRGA, LI-7500, Li-Cor, USA) (Falk et al., 2005; Ibrom et al., 2007; Panferov et al., 2009). The open-path IRGA was chosen due to its smaller power requirements compared to, e.g., closed-path sensors. The sensor was chosen to provide continuous flux measurements in the field mainly due reduced power requirements comparing with e.g. close path sensors available at that time. The sensor was calibrated with calibration gases two times per year and showed no considerable sensitivity drift within one year of operation. Turbulence data were sampled at 10 Hz and stored as raw data on an industrial mini PC (Kontron, Germany). All instruments were powered by batteries, which were charged by solar panels, mounted on the tower. The system is entirely self-sustaining

and has been proven to run unattended over a period of several months. Post-field data processing on eddy covariance flux estimates was carried out strictly according to the established recommendations for data analysis (Aubinet et al., 2012). In addition to the procedures described in Falk et al. (2005) and Ibrom et al. (2007), we corrected the flux data for CO<sub>2</sub> or H<sub>2</sub>O density fluctuations due to heat conduction from the open-path sensor -(Burba et al., 2008; Järvi et al. 2009) using finally the suggested method as described in Reverter et al. (2011).

The system operated at ca. 70% of the time. Ca. 30% of the measured flux data were negatively affected by rain and other unfavourable conditions and removed. From night time ecosystem respiration data a friction velocity ( $u_*$ ) threshold value of 0.25 m s<sup>-1</sup> was estimated (Aubinet et al., 2000), i.e. at  $u_*$  values above this threshold the measured night time flux became independent from  $u_*$ . Night time flux values that were measured at  $u_* < 0.25$  m s<sup>-1</sup> were removed, which left 15% of the measured night time flux data in the data set. For filling the gaps in the measured Net Ecosystem Exchange (NEE) and evapotranspiration, net radiation, sensible and latent heat flux records as well as to quantify GPP, RE and forest canopy transpiration the process-based Mixfor-SVAT model (Olchev et al., 2002; 2008) was used.

Mixfor-SVAT is a one-dimensional model of the energy, H<sub>2</sub>O and CO<sub>2</sub> exchange between vertically structured mono- or multi-specific forest stands and the atmosphere. The main model advantage is its ability both to describe seasonal and daily patterns of CO<sub>2</sub> and H<sub>2</sub>O fluxes at individual tree and entire ecosystem levels and to estimate the contributions of soil, different forest layers, and various tree species into the total ecosystem fluxes taking into account individual structure, biophysical properties and responses of plant species to changes in environmental conditions. The model also allows to take into account the non-steady-state water transport in the trees, rainfall interception, dew generation, turbulence and convection flows within the canopy and plant canopy energy storage. As model input the measured meteorological variables (air temperature, water vapor pressure, wind speed, precipitation, CO<sub>2</sub> concentration, global solar radiation) are used. The model was tested with long-term meteorological and flux data from different experimental sites including the investigated forest under well-developed turbulent conditions and showed a good agreement over a broad spectrum of weather and soil moisture conditions (Olchev et al., 2002; Falk et al., 2005; Falge et al., 2005; Olchev et al., 2008). Using the model is superior to common statistical gap-filling approaches, because these depend on calibration under all relevant weather conditions, including those that were systematically excluded when the open-path sensor did not work, e.g. under rain. For this reason one might argue that statistical gap-filling is biased by calibration during dry weather conditions. The process-based model is, however, able to take these weather situations into account, because it is based on general physical principles. As it was shown in previous studies the model is able to predict both CO<sub>2</sub> and water fluxes under

1 | various weather and soil moisture conditions at sites where closed-path sensors were used [Olchey  
2 | et al., 1996; Falge et al., 2005].  
3 |

#### 4 | **2.4 Micrometeorological measurements**

5 | Air temperature, relative humidity and horizontal wind speed were measured at 4 levels  
6 | above and at 2 levels inside the forest canopy using ventilated and sheltered thermo-hygrometers  
7 | and cup anemometers (Friedrichs Co., Germany) installed on the tower. Short- and long-wave  
8 | radiation components were measured below and above the canopy with CM6B and CG1 sensors  
9 | (Kipp & Zonen, The Netherlands). Rainfall intensity was measured on top of the tower with a  
10 | tipping bucket in a Hellman-type rain gauge. To fill the gaps in measuring records the  
11 | meteorological data from an autonomic meteorological station, situated about 900 m away from the  
12 | tower outside the forest on a nearby meadow, were used. For the analysis, the monthly mean values  
13 | of air temperature and monthly sums of precipitation and solar energy were calculated.  
14 |

#### 15 | **2.5 Data analysis**

16 | To estimate the possible impact of ENSO events on CO<sub>2</sub> and H<sub>2</sub>O fluxes in the tropical  
17 | rainforest at Bariri the temporal variability of monthly NEE, GPP, RE and ET in periods with  
18 | different ENSO intensity was analysed. To quantify the ENSO impacts on meteorological  
19 | parameters and fluxes and to distinguish them from effects caused by the seasonal migration of the  
20 | ITCZ, the intra-annual patterns of CO<sub>2</sub> and H<sub>2</sub>O fluxes as well as meteorological conditions during  
21 | the measuring period were also evaluated.

22 | In the first step to assess the possible impact of ENSO events on meteorological parameters  
23 | (global solar radiation (G), precipitation amount (P), air temperature (T) and CO<sub>2</sub> and H<sub>2</sub>O fluxes),  
24 | the correlation between the absolute values of monthly G, P, T, NEE, GPP, RE, ET and monthly  
25 | SST-anomalies in Nino4 and Nino3.4 regions (Nino4 and Nino3.4 indexes) were analysed.

26 | In the second step, we analyzed the correlation between the deviations of monthly  
27 | meteorological parameter and flux values from their monthly averages over the entire measuring  
28 | period and the Nino4/Nino3.4 indexes. The deviation in the case of GPP ( $\Delta GPP$ ) was estimated as

$$29 | \Delta GPP_{Month,Year} = GPP_{Month,Year} - \frac{1}{N} \sum_{Year=2004}^{2008} GPP_{Month,Year}$$

30 | where  $GPP_{Month,Year}$  is total monthly GPP for a particular month (January to December) and  
31 | corresponding year (2004 to 2008),  $\frac{1}{N} \sum_{Year=2004}^{2008} GPP_{Month,Year}$  is monthly GPP for this particular  
32 | month averaged for the entire measuring period (2004 to 2008); N is number of years. Positive

values in  $\Delta\text{GPP}$ ,  $\Delta\text{RE}$ , and  $\Delta\text{NEE}$  indicate GPP, RE higher and NEE (carbon uptake) lower than average.

The typical timescale of full ENSO cycle is estimated to be about 48-52 months (Setoh et al. 1999) whereas the timescale of the main meteorological parameters (global solar radiation (G), precipitation amount (P), air temperature (T)) is characterized by much higher month-to-month variability even after annual trend filtering. In order to filter the high-frequency oscillation in the time-series of atmospheric characteristics and monthly NEE, GPP, RE, ET anomalies the simple centered moving average smoothing procedure was applied. The moving averages (MA) of variables were calculated over 7 months (centered value  $\pm 3$  months).

Statistical analysis included both simple correlation and cross-correlation analysis (Chatfield, 2004). Cross-correlation analysis was used to take into account the possible forward and backward time shifts of maximal anomalies of meteorological parameters and CO<sub>2</sub> and H<sub>2</sub>O fluxes in respect to time of the ENSO culmination. To describe the relationships between atmospheric fluxes and meteorological parameters the monthly non-smoothed values were used.

### 3. Results

During the measuring period, two El Niño (August 2004 - March 2005 and October 2006 - January 2007) and one La Niña (November 2007 - April 2008) phenomena were observed. All events had moderate intensity. Both warm events could be classified as the Central Pacific or Modoki type, according to Ashok et al. (2007), since the SST-anomalies were centred in Nino3.4 and Nino4 regions (Figure 1).

Analysis of the intra-annual pattern of CO<sub>2</sub> and H<sub>2</sub>O fluxes shows a relatively weak seasonal variability (Figure 2). The maximal values of GPP were obtained during the second part of the drier season - from August to October ( $278 \pm 13 \text{ g C m}^{-2} \text{ month}^{-1}$ ) - which is also characterised by maximal values of incoming solar radiation. The mean monthly air temperature in the period varied from minimal values in August ( $19.2 \pm 0.2^\circ\text{C}$ ) to maximal values in October ( $19.8 \pm 0.2^\circ\text{C}$ ). The minimal GPP values were obtained in transition periods between more wet and dry seasons - in May - June and November - December ( $240 \pm 15$  and  $249 \pm 21 \text{ g C m}^{-2} \text{ month}^{-1}$ , respectively). These periods are also characterised by minimal amounts of incoming solar radiation ( $512 \pm 40 \text{ MJ m}^{-2} \text{ month}^{-1}$ ). Maximal RE ( $206 \pm 10 \text{ g C m}^{-2} \text{ month}^{-1}$ ) and values were obtained in October, which corresponds to the period of maximal air temperature and insolation. The local maximum of RE in April - May ( $199 \pm 4 \text{ g C m}^{-2} \text{ month}^{-1}$ ) is also well correlated with a small increase of the air temperature in these months. The minimal RE was observed in February and June-August ( $174 \pm 10$  and  $187 \pm 15 \text{ g C m}^{-2} \text{ month}^{-1}$ , respectively). The intra-annual pattern of ET was closely related to the

1 seasonal variability of GPP. The maximum values of ET were also observed in October ( $136 \pm 4$   
2 mm), in the month of maximal incoming solar radiation and highest values of air temperature. In  
3 spite of a large amount of precipitation and a high air temperature during the period from March to  
4 June, ET in this period was much lower than in September and October (e.g.  $105 \pm 8$  mm in April).

5 Comparisons of monthly NEE, GPP, RE, ET and absolute values of SST-anomalies in  
6 Nino4 and Nino3.4 regions (henceforth Nino4 and Nino3.4 indexes) indicate relatively low  
7 correlations. Changes of the Nino4 index can explain about 12% of the observed variability in GPP  
8 (coefficient of determination,  $r^2=0.12$  under significance level  $p<0.05$ ), 9% of RE ( $r^2=0.09$ ,  $p<0.05$ ),  
9 9% of NEE ( $r^2=0.09$ ,  $p>0.05$ ), 6% of ET ( $r^2=0.06$ ,  $p<0.05$ ) and only about 1% of transpiration (TR)  
10 ( $r^2=0.01$ ,  $p>0.05$ ). Similar values were obtained in correlation analysis for the Nino3.4 index. In the  
11 periods of El Niño peak phases (September 2004 - January 2005 and October 2006 - January 2007)  
12 the values ET and GPP tend to increase in the study area. An increase of RE was indicated only  
13 during the second El Niño event from October 2006 to January 2007. The effect of El Niño on NEE  
14 was insignificant. The effect of La Niña on CO<sub>2</sub> and H<sub>2</sub>O flux components was very small and  
15 manifested only in a slight increase of NEE.

16 Analysis of the temporal variability of the centered moving average values of  $\Delta$ GPP  
17 ( $\Delta$ GPP<sub>MA</sub>) (Figure 3) in contrast to comparisons of absolute monthly GPP indicates a relatively high  
18 correlation between  $\Delta$ GPP<sub>MA</sub> and both Nino4 ( $r^2=0.52$ ,  $p<0.05$ ) and Nino3.4 ( $r^2=0.60$ ,  $p<0.05$ )  
19 indexes. Close correlation between the intensity of ENSO events and  $\Delta$ GPP<sub>MA</sub> can be explained by  
20 the influence of ENSO initiating processes and ENSO itself on total cloud amount in the region and,  
21 as a result, on monthly sums of incoming G (Figure 4). Variability of G ( $\Delta$ G<sub>MA</sub>) is very closely  
22 correlated with Nino4 and Nino3.4 indexes ( $r^2=0.48$ ,  $p<0.05$  for both indexes) (Figure 4) and it can  
23 explain 69% of variability of GPP ( $r^2=0.69$ ,  $p<0.05$ ). The maximal deviations of  $\Delta$ GPP<sub>MA</sub> and  
24  $\Delta$ G<sub>MA</sub> from mean values (averaged for the entire measuring period) are occurring 2-3 months before  
25 the peak phase of the ENSO events (Figure 5). The maximal cross-correlation coefficients in this  
26 period reached 0.76 for  $\Delta$ G<sub>MA</sub>, and 0.86 - for  $\Delta$ GPP<sub>MA</sub>. The effect of T changes ( $\Delta$ T) on  $\Delta$ GPP is  
27 very low ( $r^2=0.01$ ,  $p>0.05$ ).

28 The correlation between  $\Delta$ T<sub>MA</sub> and Nino4, Nino3.4 indexes are relatively low ( $r^2=0.15$ ,  
29  $p>0.05$  for Nino4 and  $r^2=0.05$ ,  $p>0.05$  for Nino3.4) and it can explain the very weak correlations  
30 between  $\Delta$ RE<sub>MA</sub> and ENSO indexes ( $r^2=0.10$ ,  $p<0.05$  for Nino4 and  $r^2=0.04$ ,  $p>0.05$  for Nino3.4)  
31 (Figures 3-4). The maximal deviations of T<sub>MA</sub> and RE<sub>MA</sub> from mean values (averaged for the entire  
32 measuring period) are occurring 2 months after the peak phase of the ENSO events and it has  
33 negative sign (Figure 5). The cross-correlation coefficient in this period is -0.53 ( $p<0.05$ ).

34 Despite the relatively close dependence of  $\Delta$ GPP<sub>MA</sub> on ENSO intensity, the correlations  
35 between  $\Delta$ NEE<sub>MA</sub> and Nino4, Nino3.4 indexes are lower ( $r^2 = 0.31$ ,  $p<0.05$  for Nino4 and  $r^2 = 0.37$ ,

1 p<0.05 for Nino3.4), mainly because of their very low correlation during the first part of the  
2 measuring period (before December 2005). During the second part of the considered period (from  
3 June 2006 to June 2008) with one strong El Niño (October 2006 - January 2007) and one La Niña  
4 (November 2004 - April 2008) events  $\Delta\text{NEE}_{\text{MA}}$  and Nino4, Nino3.4 indexes are correlated much  
5 better. It can be explained by the influence of  $\Delta\text{RE}_{\text{MA}}$  on  $\Delta\text{NEE}_{\text{MA}}$  dynamics that is mainly  
6 governed by temperature variability and which is, as already mentioned, very poorly correlated with  
7 Nino4/Nino3.4 indexes (Figures 3-4).

8 Taking into account that the monthly anomalies of NEE might be biased by a still  
9 unaccounted advection effects at night-time, despite  $u^*$  filtering, we additionally examined NEE at  
10 midday (10:00-14:00), when turbulent mixing is typically well developed. Data analysis based on  
11 midday NEE shows a similar clear relationship with the ENSO index (Figure 6) with  $r^2 = 0.59$   
12 under p<0.05. The maximal deviations of both  $\text{NEE}_{\text{MA}}$  and midday  $\text{NEE}_{\text{MA}}$  from the their mean  
13 values occurred simultaneously within the peak phase of the ENSO events (Figure 5).

14 Analysis of the temporal variability of the moving average values of monthly ET ( $\Delta\text{ET}_{\text{MA}}$ )  
15 showed a high correlation to ENSO activity as well:  $r^2 = 0.72$ , p<0.05 for Nino4 and  $r^2 = 0.70$ ,  
16 p<0.05 for Nino3.4 (Figure 7), probably also triggered by  $G_{\text{MA}}$ , which in turn correlated strongly  
17 with both the Nino4 and the Nino3.4 index. Periods of extreme  $\Delta\text{ET}_{\text{MA}}$  values and maximal ENSO  
18 intensity occurred simultaneously (Figure 5). Correlations between  $\Delta\text{ET}$  and  $\Delta\text{T}$ , as well as between  
19  $\Delta\text{ET}$  and  $\Delta\text{P}$ , are insignificant -  $r^2=0.09$  (p>0.05) and  $r^2=0.01$  (p>0.05), respectively. However,  
20 figures 4 and 5 clearly show a time delay in  $\Delta\text{P}_{\text{MA}}$  oscillation, relative to Nino4 and Nino3.4  
21 patterns. The maximal negative deviations of  $\Delta\text{P}_{\text{MA}}$  are observed about eight months before (cross-  
22 correlation between  $\Delta\text{P}_{\text{MA}}$  and Nino 4 index 0.72, p<0.05) and maximal positive deviation of  $\Delta\text{P}_{\text{MA}}$   
23 - about four-five months after the peak phases of ENSO (cross-correlation between  $\Delta\text{P}_{\text{MA}}$  and Nino  
24 4 index - 0.40, p<0.05), respectively.

25 To explain a very low sensitivity of ET to P changes, we analysed the intra-annual  
26 variability of the ratio between ET and potential evaporation (PET), as well as between ET and P.  
27 PET was derived using the well-known Priestley and Taylor (1972) approach and it is equal to  
28 evaporation from wet ground or open water surface.

29 The mean annual ET during the measuring period is considerably lower than P  
30 ( $\text{ET}/\text{P}=0.742$ ). Over the annual course, the ratio varied between 0.58 (in March and November) to  
31 1.85 (in August and October). During dry periods before the positive phase of ENSO, the mean  
32 values of the ET/P ratio grow up to 1.9-2.1. During the periods of negative Nino4 and Nino3.4  
33 anomalies the mean monthly ET/P ratio fell, in some months, down to 0.3. Correlation analysis of  
34 temporal variability of  $\Delta(\text{ET}/\text{P})$  and  $\Delta(\text{ET}/\text{P})_{\text{MA}}$  ratios and Nino4 and Nino3.4 indexes (Figure 7) did  
35 not show any statistically significant relationships. However, it should be mentioned that the

1 temporal pattern of  $\Delta(\text{ET}/\text{P})$  and  $\Delta(\text{ET}/\text{P})_{\text{MA}}$  is characterised by two peaks that were observed in  
2 July of 2005 and April 2007, about 6-8 months prior to the El Niño culmination (Figure 7).

3 The monthly mean ET/PET ratio has a feeble intra-annual course with maximum in June  
4 ( $0.93 \pm 0.03$ ) and with minima in February and October ( $0.84 \pm 0.06$ ). The averaged annual ET/PET  
5 ratio for the entire measuring period was  $0.880 \pm 0.055$ . The minimal values of  $(\text{ET}/\text{PET})_{\text{MA}}$   
6 ( $(\text{ET}/\text{PET})_{\text{MA}} = 0.81$ ) were observed during the El Niño culmination in 2005-2006, and the maximal  
7 values, during the period of maximal intensity of La Niña in 2008 ( $(\text{ET}/\text{PET})_{\text{MA}} = 0.93$ ). Thus,  
8 monthly ET rates are relatively close to PET values during the whole year including the periods of  
9 maximal ENSO activity. The relative soil water content of the upper 30 cm horizon calculated using  
10 the Mixfor-SVAT model during the entire period of the field measurements, including the periods  
11 with maximal values of the ET/P ratio, was always higher than 80%. This, together with the  
12 ET/PET ratio, is a clear indicator of permanently sufficient soil moisture conditions in the study  
13 area, including periods of El Niño and La Niña culminations, explaining the very low sensitivity of  
14  $\Delta\text{ET}$  to  $\Delta\text{P}$ .

## 16 **4. Discussion**

### 17 **4.1. Uncertainty of the analysis**

18 Eddy covariance flux measurements in tropical mountainous conditions are challenging. Our  
19 tower and eddy covariance system was designed to minimise power consumption by using an open-  
20 path sensor, which had the consequence that rainy conditions systematically caused gaps in the flux  
21 data. To minimise a potential bias on the flux sums, we used a process-based forest model that is  
22 not biased by a lack of data in wet conditions as the often used statistical gap-filling algorithms  
23 (Reichstein et al., 2005, see also section 2.3). The weather in the tropics typically -has a relatively  
24 high percentage of calm nights. The selected forest is located on a plateau in a mountainous region  
25 and this increases the risk of CO<sub>2</sub> rich air draining downhill in calm night. We investigated this  
26 effect very carefully and found that the CO<sub>2</sub> fluxes showed a very clear  $u_*$  threshold above which  
27 the night time CO<sub>2</sub> emission rates did not depend on  $u_*$  anymore. Using only data from nights with  
28 sufficient turbulence ( $u_* > u_*$  threshold value) we minimised advection and drainage affecting the  
29 NEE estimates. Also, here we benefitted from the use of the process-based model for gap-filling.  
30 We then analysed the statistical relationships between our gap-filled monthly fluxes with climate  
31 anomaly indices and corroborated these analyses also with midday NEE data only. As time data are  
32 independent from night time data, we made sure that our analysis was not affected by night time  
33 flux loss. The correlations with midday data and ENSO indices were very similar to those with  
34 daily mean NEE data. This demonstrated the robustness of our analysis.

To estimate the performance of the model applied for gap-filling as it was already mentioned the model was compared with eddy covariance flux data obtained under well developed turbulent conditions. The coefficient of determination ( $r^2$ ), absolute fractional bias (AFB) and Willmott's index of agreement (IA) between modeled and measured fluxes were calculated (Olchev et al., 2008). Comparisons showed a relatively good agreement between the modeled and measured  $\text{H}_2\text{O}$  and  $\text{CO}_2$  fluxes. In particular the determination coefficients ranged between 0.62 for  $\text{CO}_2$  to 0.64 for  $\text{H}_2\text{O}$  fluxes Calculated AFBs were about 0.52 for  $\text{CO}_2$  and about 0.54 for  $\text{H}_2\text{O}$  fluxes. Both values are located within a critical interval of AFB (between 0 and 0.67). Willmott's indexes of agreement indicating the degree to which model predictions are error free were about 0.87 for  $\text{CO}_2$  and about 0.86 for  $\text{H}_2\text{O}$  fluxes that also indicates a good agreement of the model and field data.

In addition we compared the model predicted mean annual soil respiration rate with soil  $\text{CO}_2$  efflux data that were measured in the study region with soil chambers (van Straaten et al. 2011). The Mixfor-SVAT model estimated an average annual soil respiration rate of  $1110 \pm 30 \text{ g C m}^{-2} \text{ yr}^{-1}$  for the investigated site. This value was very close to the measured average soil  $\text{CO}_2$  efflux of for the central Sulawesi region of  $1170 \text{ g C m}^{-2} \text{ yr}^{-1}$  which shows realistic behavior of the model.

The relatively high annual NEE sums need further investigation. After applying all corrections including the correction for open-path sensor heating and after gap filling we found an average annual uptake of  $729 \pm 32 \text{ g C m}^{-2} \text{ yr}^{-1}$  (standard deviation between 5 different years). This value is higher as the range found in lowland rain forests, i.e. ranging from e.g. 75 to 538  $\text{g C m}^{-2} \text{ yr}^{-1}$ .(Luyssaert et al., 2007). The clarification of this very interesting phenomenon, maybe relating to the site history and regrowth after selected use of large individual trees by the local population, lies however not within the scope of this article.

## 4.2 Effects of large scale climate anomalies on carbon and water exchange in the investigated site

The provided analysis of the temporal variability for the main components of carbon and water balances in the tropical rainforest showed a high correlation between Nino4 and Nino3.4 SST anomalies, characterising the ENSO intensity with  $\Delta\text{GPP}_{\text{MA}}$ ,  $\text{GPP}_{\text{MA}}$  and  $\Delta\text{ET}_{\text{MA}}$  over the entire measuring period. The Application of the centered moving average smoothing procedure allowed us to filter the high-frequency month-to-month oscillations in the time-series of atmospheric characteristics. These are caused by local and regional circulation processes that are not directly connected with ENSO activity and disturb thus the analysis. The relationships between  $\Delta\text{GPP}_{\text{MA}}$ ,  $\Delta\text{ET}_{\text{MA}}$  and Nino4 and Nino3.4 indexes are mainly governed on the one hand by via the dependency of the incoming solar radiation on ENSO development – surface water warming in Nino 3.4 and 4 regions generally results in a

decrease of cloudiness above the study region and thus —in an increase of incoming solar radiation. On the other hand there are many data about a The high correlation between of monthly GPP and ET rates and with incoming and absorbed solar radiation at this site is well described (e.g. Ibrom et al., 2008). The effects of monthly air temperature and precipitation changes on  $\Delta\text{GPP}$  and  $\Delta\text{ET}$  variability are on the contrary relatively poor, mainly due to the low correlations between  $\Delta T_{\text{MA}}$ ,  $\Delta P_{\text{MA}}$  and ENSO intensity are not very much related.

The cross-correlation analysis (Fig. 5) shows that the  $\Delta\text{GPP}_{\text{MA}}$  and  $\Delta\text{G}_{\text{MA}}$  have a small 2-3 month backward shift relatively to the course of Nino4 SST, i.e. the maxima in  $\text{GPP}_{\text{MA}}$  occur earlier than ENSO culmination in the central Pacific (Nino4 SST anomaly). The maximal values of  $\Delta E_{\text{MA}}$  occurred simultaneously with El Niño and La Niña culminations. Such an effect of El Niño episodes on G can be explained, as mentioned above, by a decrease of the cloud amount cover in the region of Indonesia, due to the El Niño-associated shift of the Walker circulation cell, and corresponding zone of deep convection, from the maritime continent of Indonesia toward the dateline following SST anomalies displacement. El Niño usually begins in April, and toward August-September the ascending branch of the Walker cell leaves Indonesia and migrates eastward to the Pacific. Therefore, 3-4 months before the El Niño culmination in December-January, a decrease in cloud amount is observed over Indonesia. Weakening of El Niño, in turn, leads to a backward shift of intensive convection zone westward. It can result in increasing precipitation amounts in the region during the second half of the wet period after passing the maximal El Niño activity and also the gradual increase of the cloudiness and decrease of incoming solar radiation. The opposite effect takes place during the La Niña with similar phase shift: simultaneously, with the spreading of a negative SST anomaly over the Pacific, the increasing of deep convection over Indonesia occurs, which results in an increase of cloudiness and precipitation, being more pronounced as it falls into the dry period of the year. The lower panels of Figure 4 indicate however, that the decrease of radiation due to increase of cloudiness does not depend linearly on La Niña intensity, reaching a saturation state at approximately  $-20..-30 \text{ MJ m}^{-2} \text{ month}^{-1}$ .

A relatively poor correlation between  $\Delta T_{\text{MA}}$  patterns and ENSO activity and an insignificant influence of  $\Delta T$  on  $\Delta\text{GPP}$  and  $\Delta\text{ET}$  can be mainly explained by the small intra-annual amplitude of the air temperature in the study area not exceeding  $1.0^{\circ}\text{C}$ , as well as by the low dependence of the air temperature on incoming solar radiation. The mean monthly temperatures ranged in the intra-annual course between  $19.5^{\circ}\text{C}$  and  $20.5^{\circ}\text{C}$ . Maximal air temperatures do not exceed  $28.5^{\circ}\text{C}$ , even on sunny days. Such optimal thermal conditions with high precipitation amount provide sufficient soil moistening and relatively comfortable conditions for tree growth during the whole year. As is was already mentioned even during the El Niño culmination in 2005-2006 the ET/PET did not

1 decrease below 0.74,  $(ET/PET)_{MA} > 0.81$ , and the relative soil water content of the upper 30 cm  
2 horizon was always higher than 80%.

3 The analysis of absolute and relative changes of GPP and ET during the periods of maximal  
4 El Niño and La Niña activities showed that GPP during the El Niño culminations of 2005 and 2007  
5 increased by about  $20 \text{ g C m}^{-2} \text{ month}^{-1}$  (6-7%).  $\Delta GPP_{MA}$  was about  $9 \text{ g C m}^{-2} \text{ month}^{-1}$  (2-3%),  $\Delta ET$   
6 - about  $40 \text{ mm month}^{-1}$  (about 30%) and  $\Delta ET_{MA}$  - about  $10 \text{ mm month}^{-1}$  (6-7%). Thus, the maximal  
7  $\Delta GPP$  was two times lower than the mean annual amplitude of GPP (Figure 2). The maximal  $\Delta ET$   
8 was equal to the annual amplitude of ET (Figure 2). During the La Niña culmination of 2008 the  
9 maximal relative changes of GPP were higher than the relative changes observed during El Niño  
10 events:  $\Delta GPP$  was about  $-22 \text{ g C m}^{-2} \text{ month}^{-1}$  (8%),  $\Delta GPP_{MA}$  - about  $-12 \text{ g C m}^{-2} \text{ month}^{-1}$  (4%). The  
11 maximal decrease of  $\Delta ET$  in the period was relatively small:  $\Delta ET$  - about  $-12 \text{ mm month}^{-1}$  (10%)  
12 and  $\Delta ET_{MA}$  - about  $-5 \text{ mm month}^{-1}$  (4%).  $\Delta ET$  was about 3 times lower than the mean annual  
13 amplitude of ET. Interestingly the radiation dependent GPP (as represented by smoothed 7 month  
14 mean) does not demonstrate any prolonged constant period during La Niña phases though the  
15 radiation does. During the first cold event the GPP-reduction is not as strong as during the second  
16 one, although the G-reductions are nearly of same strength. It could be assumed that in the first case  
17 the effect of radiation decrease on GPP was compensated by other factors like slight increase of the  
18 air temperature.

19 Additionally, we investigated the influence of other climatic anomalies in the region on  $\text{CO}_2$   
20 and  $\text{H}_2\text{O}$  fluxes of the tropical rainforest, such as the Madden–Julian oscillation (MJO) and the  
21 Indian Ocean Dipole (IOD). The MJO is characterised by an eastward propagation of large regions  
22 of enhanced and suppressed deep convection from the Indian ocean toward central Pacific (Zhang,  
23 2005). Each MJO cycle lasts approximately 30–60 days and includes wetter (positive) and drier  
24 (negative) phases. As an estimation of deep convection intensity in the tropics, the outgoing long-  
25 wave radiation (OLR) measured at the top of the atmosphere is commonly used. It was recently  
26 shown that 6–12 months prior to the onset of an El Niño episode a drastic intensification of the MJO  
27 occurs in the Western Pacific (Zhang and Gottschalck, 2002; Lau, 2005; Hendon et al., 2007;  
28 Gushchina and Dewitte, 2011). Furthermore, MJO behaviour varies significantly during the ENSO  
29 cycle: it is significantly decreased during the maxima of conventional El Niño episodes, while it is  
30 still active during the peak phase of central Pacific events. MJO rarely occurs during La Niña  
31 episodes (Gushchina and Dewitte, 2012). As MJO is strongly responsible for intra-seasonal  
32 variation of precipitation in the study region, the occurrence of MJO events was compared to the  
33 significant anomalies of ET/P ratio and of key meteorological variables. No evidence of MJO  
34 influence is observed: the positive and negative anomalies of ET/P ratio are associated to positive,

negative and zero anomalies of OLR, filtered in the MJO interval. Also, no significant relation emerged from the correlation analysis.

Correlations between MJO index (Wheeler and Kiladis, 1999; Gushchina and Dewitte, 2011), and the deviations of key meteorological parameters from monthly averages during the study period were very low:  $r^2 = 0.03$  for T,  $r^2 = 0.03$  for P and  $r^2 = 0.01$  for G ( $p > 0.05$ , in ~~both all~~ cases).

The Indian Ocean Dipole (IOD) is characterised by changes of the SST in the western Indian Ocean, resulting in intensive rainfall in the western part of Indonesia during the positive phase and corresponding precipitation reduction during the negative phase (Saji et al., 1999). To find a possible influence of IOD events on temporal variability of meteorological parameters and CO<sub>2</sub> and H<sub>2</sub>O fluxes, the monthly mean IOD index (Dipole Mode Index, DMI) was used. Results showed that with respect to the western part of Indonesia situated close to Indian Ocean the IOD phenomenon has no significant impact on meteorological conditions and fluxes of the area of Central Sulawesi.

Our case study showed a high sensitivity of the main components of CO<sub>2</sub> and H<sub>2</sub>O fluxes of the investigated mountainous tropical rainforest in Bariri to El Niño and La Niña phenomena as well as a low sensitivity to IOD and MJO events. The time lag between the respective indices and their effect on the fluxes at our site indicates that the timing and the extent of the effects are site specific. The fluxes respond to the local weather and only indirectly to the large scale weather anomalies, i.e. in the way the local weather is affected by the large scale weather phenomena. The observed phenomena are thus not representative for all mountainous forest sites in the tropics. The conclusion is that large scale weather anomalies do have systematic effects on local fluxes but the timing and the extent are likely to differ across different regions.

Even though remote sensing analyses have shown that the site is representative for the region (Ibrom et al. 2007, Popastin et al. 2012), the response to ENSO might differ in the region due to differences in altitude and land-use (Erasmi et al. 2009). In general, anthropogenic deforestation has removed most parts of lowland forests so that the remaining forest cover consists mostly of mountainous forests. At the moment, there are no other FLUXNET sites situated in equatorial mountainous rainforests of South-East Asia with which we could directly compare our findings and investigate whether similar response to ENSO can be observed. Most of the existing FLUXNET sites (AsiaFlux) are not comparable with the investigated site as they are situated in subequatorial and tropical climate zones. These are characterized by higher seasonality of air temperature and precipitation compared to our equatorial site. Thus, our site provides a unique opportunity to investigate the response of an equatorial mountainous rainforest to ENSO in the Western pacific region.

1    **5. Conclusions**

2       CO<sub>2</sub> and H<sub>2</sub>O fluxes in the mountainous tropical rainforest in Central Sulawesi in Indonesia  
3       showed a high sensitivity of monthly GPP and ET to ENSO intensity for the period from January  
4       2004 to June 2008. This was mainly governed by the high dependency of incoming solar radiation  
5       ( $G$ ) to Nino4 and Nino3.4 SST changes and the strong sensitivity of GPP and ET on  $G$ .

6       Interestingly, we observed time shifts between the SST anomalies and smoothed GPP  
7       anomalies driven by radiation anomalies. The maximal deviations of GPP and  $G$  from their mean  
8       values occurred 2-3 months before the peak phase of the ENSO events. The effect of ENSO  
9       intensity on ecosystem respiration, RE, was relatively low, mainly due to its weak effect on air  
10      temperature. Anyway, the small cross-correlation between RE and ENSO intensity had a  
11      compensatory effect on the respective timing of NEE, which thus was - like evapotranspiration - in  
12      synchrony with El Niño culminations. -Unlike the observations in other tropical sites, precipitation  
13      variations had no influence on the CO<sub>2</sub> and H<sub>2</sub>O fluxes at study site, mainly due to the permanently  
14      sufficient soil moisture condition in the study area.

15      Other climatic anomalies in the Western Pacific region, such as the Indian Ocean Dipole and  
16      the Madden–Julian oscillation, did not show any significant effect on neither the meteorological  
17      conditions nor the CO<sub>2</sub> and H<sub>2</sub>O fluxes in the investigated mountainous-tropical-rainforest in  
18      Central Sulawesi.

19      It is important to emphasise that the considered-observation period does not cover any  
20      period with extreme El Niño events, such as, e.g., the 1982-83 and 1997-98 events, when the  
21      anomaly of Nino3.4 SST, during several months, exceeded 2.6°C and more significant changes of  
22      surface water availability were observed. Also, in lowland parts of Sulawesi, characterised by  
23      higher temperatures and lower precipitation, the vegetation response to ENSO events is likely to be  
24      different and more pronounced (Erasmi et al., 2009).

25      All observed ENSO events during the selected period are classified as Central Pacific type.  
26      Recently, Yeh et al. (2009) showed that under projected climate change the proportion of Central  
27      Pacific ENSO events might increase. Furthermore, Cai et al. (2014, 2015) showed that current  
28      projections of climate change for the 21<sup>st</sup> century suggest an increased future likelihood of both El  
29      Niño and La Niña events. Based on the results of our study, potential increases in ENSO activity  
30      would result in an increased variability of the CO<sub>2</sub> and H<sub>2</sub>O exchange between atmosphere and the  
31      tropical rainforests in such-these and similar regions.

32

33    **Acknowledgement**

The study was supported by the German [ResearchScience](#) Foundation under the projects "Stability of Rainforest Margins in Indonesia", STORMA (SFB 552), "Ecological and Socioeconomic Functions of Tropical Lowland Rainforest Transformation Systems (Sumatra, Indonesia)" (SFB 990) and KN 582/8-1. The Russian Science Foundation (grant RSCF 14-27-00065) supports A. Olchev in part of the model development.

## Reference

1. Aiba, S., and Kitayama, K.: Effects of the 1997-98 El Niño drought on rain forests of Mount Kinabalu, Borneo, *Journal of Tropical Ecology*, 18, 215–230, 2002
2. Ashok, K., Behera, S. K., Rao S. A., Weng H., Yamagata, T.: El Niño Modoki and its possible teleconnection. *J. Geophys. Res.* 112, C11007, doi:10.1029/2006JC003798, 2007
3. Ashok, K. and Yamagata, T.: The El Niño with a difference. *Nature*, 461, 481-484, 2009
4. Aubinet, M., A. Grelle, A. Ibrom, U. Rannik, J. Moncrieff, T. Foken, A. S. Kowalski, P. H. Martin, P. Berbigier, C. Bernhofer, R. Clement, J. Elbers, A. Granier, T. Grunwald, K. Morgenstern, K. Pilegaard, C. Rebmann, W. Snijders, Valentini R. and Vesala T.: Estimates of the annual net carbon and water exchange of forests: The EUROFLUX methodology. *Advances In Ecological Research*, 30, 113-175, 2000
5. Aubinet, M., Vesala, T., and Papale, D. (Eds.): *Eddy Covariance: A Practical Guide to Measurement and Data Analysis*. Springer Atmospheric Sciences, Springer Verlag, Dordrecht, The Netherlands, 438 pp., 2012
6. Burba, G.G., McDermitt, D.K., Grelle, A., Anderson, D.J., Xu, L.: Addressing the influence of instrument surface heat exchange on the measurements of CO<sub>2</sub> flux from open-path gas analyzers. *Global Change Biology*, 14, 1-23, 2012
7. Cai, W., Borlace, S., Lengaigne, M., van Renssch, P., Collins, M., Vecchi, G., Timmermann, A., Santoso, A., McPhaden, M.J., Wu, L., England, M.H., Wang, G., Guilyardi, E. and Jin, F.-F.: Increasing frequency of extreme El Niño events due to greenhouse warming. *Nature Climate Change*, 4, 111-116, 2014
8. Cai, W., Wang, G., Santoso, A., McPhaden, M., Wu, L., Jin, F-F., Timmermann, A., Collins, M., Vecchi, G., Lengaigne, M., England, M., Dommenget, D., Takahashi, K., Guilyardi, E.: More frequent extreme La Niña events under greenhouse warming. *Nature Climate Change*, 5, 132-137, 2015
9. Chatfield, C.: *The Analysis of Time series, An Introduction*, sixth edition. Chapman & Hall/CRC, New York, 333 pp., 2004

- 1 10. Chen, D. and Chen, H. W.: Using the Koppen classification to quantify climate variation and  
2 change: An example for 19012010. *Environmental Development*, 6, 69-79, 2013
- 3 11. Ciais, P., Piao, S.L., Cadule, P., Friedlingstein, P., and Chedin, A.: Variability and recent trends  
4 in the African terrestrial carbon balance. *Biogeosciences*, 6, 1935-1948, 2009
- 5 12. Clark, D.A., and Clark, D.B.: Climate-induced variation in canopy tree growth in a Costa Rican  
6 tropical rain forest. *Journal of Ecology*, 82, 865-872, 1994
- 7 13. Download Climate Timeseries: [http://www.esrl.noaa.gov/psd/gcos\\_wgsp/Timeseries/](http://www.esrl.noaa.gov/psd/gcos_wgsp/Timeseries/), 24 April  
8 2013
- 9 14. Erasmi, S., Propastin, P., Kappas, M., and Panferov, O.: Patterns of NDVI variation over  
10 Indonesia and its relationship to ENSO during the period 1982-2003, *J Climate*, 22(24), 6612–  
11 6623, 2009
- 12 15. Falge, E., Reth, S., Brüggemann, N., Butterbach-Bahl, K., Goldberg, V., Oltchev, A., Schaaf,  
13 S., Spindler, G., Stiller, B., Queck, R., Köstner, B., Bernhofer, C.: Comparison of surface  
14 energy exchange models with eddy flux data in forest and grassland ecosystems of Germany. *J.  
15 Ecological Modelling*, 188 (2-4), 174-216, 2005
- 16 16. Falk U., Ibrom A., Kreilein H., Oltchev A., and Gravenhorst, G.: Energy and water fluxes  
17 above a cacao agroforestry system in Central Sulawesi, Indonesia, indicate effects of land-use  
18 change on local climate *Met. Zeitsch.*, 14(2), 219-225, 2005
- 19 17. FAO: Global forest resources assessment 2010: Main report, FAO Forestry Paper 163, Rome,  
20 Italy, 340 pp., 2010
- 21 18. Feely, R.A., Wanninkhof, R., Takahashi, T., and Tans, P.: Influence of El Niño on the  
22 equatorial Pacific contribution to atmospheric CO<sub>2</sub> accumulation. *Nature* 398, 597-601, 1999
- 23 19. Fisher, J.B., Sikka, M., Sitch, S., Ciais, P., Poulter, B., Galbraith, D., Lee, J.-E., Huntingford,  
24 C., Viovy, N., Zeng, N., Ahlstrom, A., Lomas, M.R., Levy, P.E., Frankenberg, C., Saatchi, S.,  
25 and Malhi, Y.: African tropical rainforest net carbon dioxide fluxes in the twentieth century.  
26 *Phil Trans R Soc B*, 368, 20120376, <http://dx.doi.org/10.1098/rstb.2012.0376>, 2013
- 27 20. Gerold, G., Leemhuis, C.: Effects of “ENSO-events” and rainforest conversion on river  
28 discharge in Central Sulawesi (Indonesia). In: *Tropical Rainforests and Agroforests under  
29 Global Change Environmental Science and Engineering*, T. Tscharntke, Ch. Leuschner, E.  
30 Veldkamp, H. Faust, E. Guhardja, A. Bidin (Eds), 327-350, 2010
- 31 21. Grace, J., Lloyd, J., McIntyre, J., Miranda, A., Meir, P., Miranda, H., Nobre, C., Moncrieff,  
32 J.B., Massheder, J.M., Malhi, Y., Wright, I., and Gash, J.C.: Carbon dioxide uptake by an  
33 undisturbed tropical rain forest in south-west Amazonia, 1992 to 1993. *Science*, 270, 778-780,  
34 1995

- 1 22. Grace, J., Malhi, Y., Lloyd, J., McIntyre, J., Miranda, A.C., Meir, P., and Miranda, H.S.: The  
2 use of eddy covariance to infer the net carbon uptake of Brazilian rain forest. *Global Change*  
3 *Biology*, 2, 209-218, 1996
- 4 23. Graf, H.-F., and Zanchettin, D.: Central Pacific El Niño, the “subtropical bridge,” and Eurasian  
5 climate, *J. Geophys. Res.*, 117, D01102, doi:10.1029/2011JD016493, 2012
- 6 24. Gushchina, D., and Dewitte, B.: The relationship between intraseasonal tropical variability and  
7 ENSO and its modulation at seasonal to decadal timescales, *Cent. Eur. J. Geosci.*, 1(2), 175-  
8 196, 2011, DOI: 10.2478/s13533-011-0017-3
- 9 25. Gushchina, D., and Dewitte, B.: Intraseasonal tropical atmospheric variability associated to the  
10 two flavors of El Niño. *Month. Wea. Rev.*, 140, (11). 3669-3681, 2012
- 11 26. Hansen, M.C., Potapov, P. V., Moore, R., Hancher, M., Turubanova, S.A., Tyukavina, A.,  
12 Thau, D., Stehman, S.V., Goetz, S.J., Loveland, T.R., Komardeey, A. Egorov, A., Chini, L.,  
13 Justice, C.O., and Townshend, J.R.G.. High-Resolution Global Maps of 21st-Century Forest  
14 Cover Change. *Science*, 342, 850-853, 2013
- 15 27. Hirano, T., Segah, H., Harada, T., Limin, S., June, T., Hirata, R., and Osaki, M.: Carbon  
16 dioxide balance of a tropical peat swamp forest in Kalimantan, Indonesia. *Global Change*  
17 *Biology*, 13, 412–425. doi: 10.1111/j.1365-2486.2006.01301.x, 2007
- 18 28. Ibrom, A., Olchev, A., June, T., Ross, T., Kreilein, H., Falk, U., Merklein, J., Twele, A.,  
19 Rakkibu, G., Grote, S., Rauf, A., and Gravenhorst, G.: Effects of land-use change on matter and  
20 energy exchange between ecosystems in the rain forest margin and the atmosphere. In *The*  
21 *stability of tropical rainforest margins: Linking ecological, economic and social constraints.*  
22 Eds. T. Tscharntke, C. Leuschner, M. Zeller, E. Guhardja and A. Bidin, Springer Verlag,  
23 Berlin, pp. 463 – 492, 2007
- 24 29. Ibrom, A., Oltchev, A., June, T., Kreilein, H., Rakkibu, G., Ross, Th., Panferov, O.,  
25 Gravenhorst, G.: Variation in photosynthetic light-use efficiency in a mountainous tropical rain  
26 forest in Indonesia. *Tree Physiology*, 28(4), 499–508, 2008
- 27 30. Järvi, L., Mammarella, I., Eugster, W., Ibrom, A., Siivola, E., Dellwik, E., Keronen, P., Burba,  
28 G., Vesala, T.: Comparison of net CO<sub>2</sub> fluxes measured with open- and closed-path infrared gas  
29 analyzers in urban complex environment. *Boreal Environmental Research*, 14, 499–514, 2009
- 30 31. Kug, J.-S., Jin, F.-F., and An, S.-I.: Two types of El Niño events: Cold tongue El Niño and  
31 warm pool El Niño, *J. Climate*, 22, 1499–1515, 2009
- 32 32. Larkin, N. K., and Harrison, D.E.: Global seasonal temperature and precipitation anomalies  
33 during El Niño autumn and winter. *Geophysical Research Letters*, 32, L13705, 2005,  
34 doi:10.1029/2005GL022738.

- 1    33. Lau, W. K. M.: El Niño Southern Oscillation connection. Intraseasonal Variability of the  
2    Atmosphere-Ocean Climate System, W. K. M. Lau, and D. E. Waliser., Eds., Praxis  
3    Publishing, Chichester, UK, 271-300, 2005
- 4    34. Lewis, S.L., Lopez-Gonzalez, G., Sonke, B., Affum-Baffoe, K., Baker, T.R., Ojo, L.O.,  
5    Phillips, O.L., Reitsma, J.M., White, L., Comiskey, J.A., Djuikouo, K. M.-N., Ewango, C.E.N.,  
6    Feldpausch, T.R., Hamilton, A.C., Gloor, M., Hart, T., Hladik, A., Lloyd, J., Lovett, J.C.,  
7    Makana, J.-R., Malhi, Y., Mbago, F.M., Ndangalasi, H.J., Peacock, J., Peh, K. S.-H., Sheil, D.,  
8    Sunderland, T., Swaine, M.D., Taplin, J., Taylor, D., Thomas, S.C., Votere, R. and Woll, H.:  
9    Increasing carbon storage in intact African tropical forests. Nature, 457: 1003-1006, 2009
- 10    34.35. Luyssaert, S., Inglima, I., Jung, M., Richardson, A.D., Reichstein, M., Papale, D., Piao, S.L., Schulze, E.-D., Wingate, L., Matteucci, G., Aragao, L., Aubinet, M., Beer, C., Bernhofer, C., Black, K.G., Bonal, D., Bonnefond, J.-M., Chambers, J., Ciais, P., Cook, B., Davis, K.J., Dolman, A.J., Gielen, B., Goulden, M., Grace, J., Granier, A., Grelle, A., Griffis, T., Grünwald, T., Guidolotti, G., Hanson, P.J., Harding, R., Hollinger, D.Y., Hutyra, L.R., Kolari, P., Kruijt, B., Kutsch, W., Lagergren, F., Laurila, T., Law, B.E., Le Maire, G., Lindroth, A., Loustau, D., Malhi, Y., Mateus, J., Migliavacca, M., Misson, L., Montagnani, L., Moncrieff, J., Moors, E., Munger, J.W., Nikinmaa, E., Ollinger, S.V., Pita, G., Rebmann, C., Roupsard, O., Saigusa, N., Sanz, M.J., Seufert, G., Sierra C., Smith, M.-L., Tang, J., Valentini, R., Vesala T. and Janssens, I.A.: CO<sub>2</sub> balance of boreal, temperate, and tropical forests derived from a global database. Global Change Biology 13(12), 2509-2537, 2007
- 21    35.36. Malhi, Y., Baldocchi, D.D., and Jarvis, P.G.: The carbon balance of tropical, temperate and  
22    boreal forests. Plant Cell and Environment, 22, 715-740, 1999
- 23    36.37. Malhi, Y.: The carbon balance of tropical forest regions, 1990–2005, Current Opinion in  
24    Environmental Sustainability, 2(4), 237–244, 2010
- 25    37.38. Moser, G., Schuldt, B., Hertel, D., Horna, V., Coners, H., Barus, H., and Leuschner, C.:  
26    Replicated throughfall exclusion experiment in an Indonesian perhumid rainforest: wood  
27    production, litter fall and fine root growth under simulated drought. Global Change Biology,  
28    20, 1481–1497, doi: 10.1111/gcb.12424, 2014
- 29    39. Oltchev, A., Constantin, J., Gravenhorst, G., Ibrom, A., Heimann, J., Schmidt, J., Falk, M., Morgenstern, K., Richter, I. and Vygodskaya, N. Application of a six-layer SVAT model for simulation of evapotranspiration and water uptake in a spruce forest. Physics and Chemistry of the Earth, 21(3), 195-199, 1996
- 33    38.40. Oltchev, A., Cermak, J., Nadezhina, N., Tatarinov, F., Tishenko, A., Ibrom, A.,  
34    Gravenhorst, G.: Transpiration of a mixed forest stand: field measurements and simulation  
35    using SVAT models. J. Boreal Environmental Reserach, 7(4), 389-397, 2002

- 1 | 39.41. Olchev, A., Ibrom, A., Ross, T., Falk, U., Rakkibu, G., Radler, K., Grote, S., Krelein, H.,  
2 | and Gravenhorst G.: A modelling approach for simulation of water and carbon dioxide  
3 | exchange between multi-species tropical rain forest and the atmosphere. J. Ecological  
4 | Modelling, 212, 122–130, 2008
- 5 | 40.42. Panferov, O., Ibrom, I., Krelein, H., Oltchev, A., Rauf, A., June, T., Gravenhorst, G. and  
6 | Knohl, A.: Between deforestation and climate impact: the Bariri Flux tower site in the primary  
7 | montane rainforest of Central Sulawesi, Indonesia. The Newsletter of FLUXNET 2(3), 17-19,  
8 | 2009
- 9 | 43.. Phillips, O.L., Aragao, L., Lewis, S.L., Fisher, J.B., Lloyd, J., Lopez-Gonzalez, G., Malhi, Y.,  
10 | Monteagudo, A., Peacock, J., Quesada, C.A., van der Heijden, G., Almeida, S., Amaral, I.,  
11 | Arroyo, L., Aymard, G., Baker, T.R., Banki, O., Blanc, L., Bonal, D., Brando, P., Chave, J., de  
12 | Oliveira, A.C.A., Cardozo, N.D., Czimczik, C.I., Feldpausch, T.R., Freitas, M.A., Gloor, E.,  
13 | Higuchi, N., Jimenez, E., Lloyd, G., Meir, P., Mendoza, C., Morel, A., Neill, D.A., Nepstad,  
14 | D., Patino, S., Penuela, M.C., Prieto, A., Ramirez, F., Schwarz, M., Silva, J., Silveira, M.,  
15 | Thomas, A.S., ter Steege, H., Stropp, J., Vasquez, R., Zelazowski, P., Davila, E.A., Andelman,  
16 | S., Andrade, A., Chao, K.-J., Erwin, T., Di Fiore, A., Honorio, C. E., Keeling, H., Killeen, T.J.,  
17 | Laurance, W.F., Cruz, A.P., Pitman, N.C.A., Vargas, P.N., Ramirez-Angulo, H., Rudas, A.,  
18 | Salamao, R., Silva, N., Terborgh, J. and Torres-Lezama, A.: Drought sensitivity of the Amazon  
19 | rainforest. Science 323, 1344-1347, 2009
- 20 | 41.44. Propastin, P., Ibrom, A., Erasmi, S. and Knohl, A.: Effects of canopy photosynthesis  
21 | saturation on the estimation of gross primary productivity from MODIS data in a tropical  
22 | forest. Remote Sensing of Environment 121, 252–260, 2012
- 23 | 42.45. Setoh, T., Imawaki, S., Ostrovskii, A. and Umatani S.: Interdecadal Variations of ENSO  
24 | Signals and Annual Cycles Revealed by Wavelet Analysis. Journal of Oceanography, 55, 385-  
25 | 394, 1999
- 26 | 43.46. Priestley, C.H.B., and Taylor, R.J.: On the assessment of surface heat flux and evaporation  
27 | using large-scale parameters. Monthly Weather Review, 100 (2), 81-92, 1972
- 28 | 44.47. Rasmusson, E.M., and Carpenter, T.H.: Variations in tropical sea surface temperature and  
29 | surface wind fields associated with the Southern Oscillation/ El Niño. Monthly Weather  
30 | Review, 110, 354-384, 1982
- 31 | 45.48. Rayner, P. J., and Law, R. M.: The relationship between tropical CO<sub>2</sub> fluxes and the El  
32 | Niño-Southern Oscillation, Geophys. Res. Lett., 26(4), 493–496, doi:10.1029/1999GL900008,  
33 | 1999
- 34 | 46.49. Reichstein, M., Bahn, M., Ciais, P., Frank, D., Mahecha, M.D., Seneviratne, S.I.,  
35 | Zscheischler, J., Beer, C., Buchmann, N., Frank, D.C., Papale, D., Rammig, A., Smith, P.,

1 Thonicke, K., van der Velde, M., Vicca, S., Walz, A., Wattenbach, M.: Climate extremes and  
2 the carbon cycle. *Nature*, 500, 287–295, 2013

3 | 47.50. Reverter, B.R., Carrara, A., Fernández, A., Gimeno, C., Sanz, M.J., Serrano-Ortiz, P.,  
4 Sánchez-Cañete, E.P., Were, A., Domingo, F., Resco, V., Burba, G.G., Kowalski, A.S.:  
5 Adjustment of annual NEE and ET for the open-path IRGA self-heating correction: Magnitude  
6 and approximation over a range of climate. *Agricultural and Forest Meteorology*, 151(12),  
7 1856–1861, 2011

8 | 51. Saji, N. H., Goswami, B. N., Vinayachandran, P. N., Yamagata, T.: A dipole mode in the  
9 tropical Indian Ocean. *Nature*, 401, 360–363, 1999

10 | 48.52. van Straaten, O., Veldkamp, E., Corre, M.D.: Simulated drought reduces soil CO<sub>2</sub> efflux and  
11 production in a tropical forest in Sulawesi, Indonesia. *Ecosphere*, 2, art119, 2011

12 | 49.53. Wang, C.: Atmospheric circulation cells associated with the El Niño-Southern Oscillation. *J.*  
13 *Climate*, 15, 399–419, 2002

14 | 50.54. Wheeler, M. C., and Kiladis, G. N.: Convectively coupled equatorial waves: Analysis of  
15 clouds and temperature in the wavenumber–frequency domain. *J. Atmos. Sci.*, 56, 374–399,  
16 1999.

17 | 55. Yeh, S.-W., Kug, J.-S., Dewitte, B., Kwon, M.-H., Kirtman, B., and Jin, F.-F.: El Niño in a  
18 changing climate. *Nature*, 461, 511–514, 2009

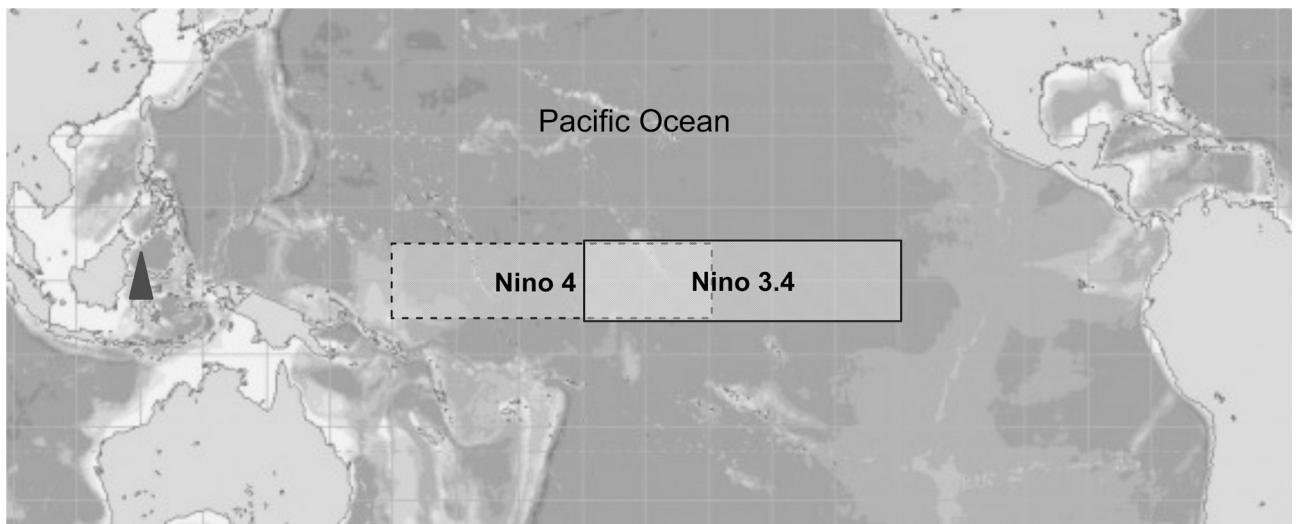
19 | 51.56. Yuan, Y. and Yan H.: Different types of La Niña events and different responses of the  
20 tropical atmosphere. *Chinese Science Bulletin* 58, 406–415, 2013

21 | 52.57. Zhang, C.: Madden-Julian Oscillation. *Reviews of Geophysics*, 43, RG2003, 2005, doi:  
22 10.1029/2004RG000158.

23 | 53.58. Zhang, C., and Gottschalck, J.: SST Anomalies of ENSO and the Madden–Julian oscillation  
24 in the equatorial Pacific. *J. Climate*, 15, 2429–2445, 2002

25

1  
2

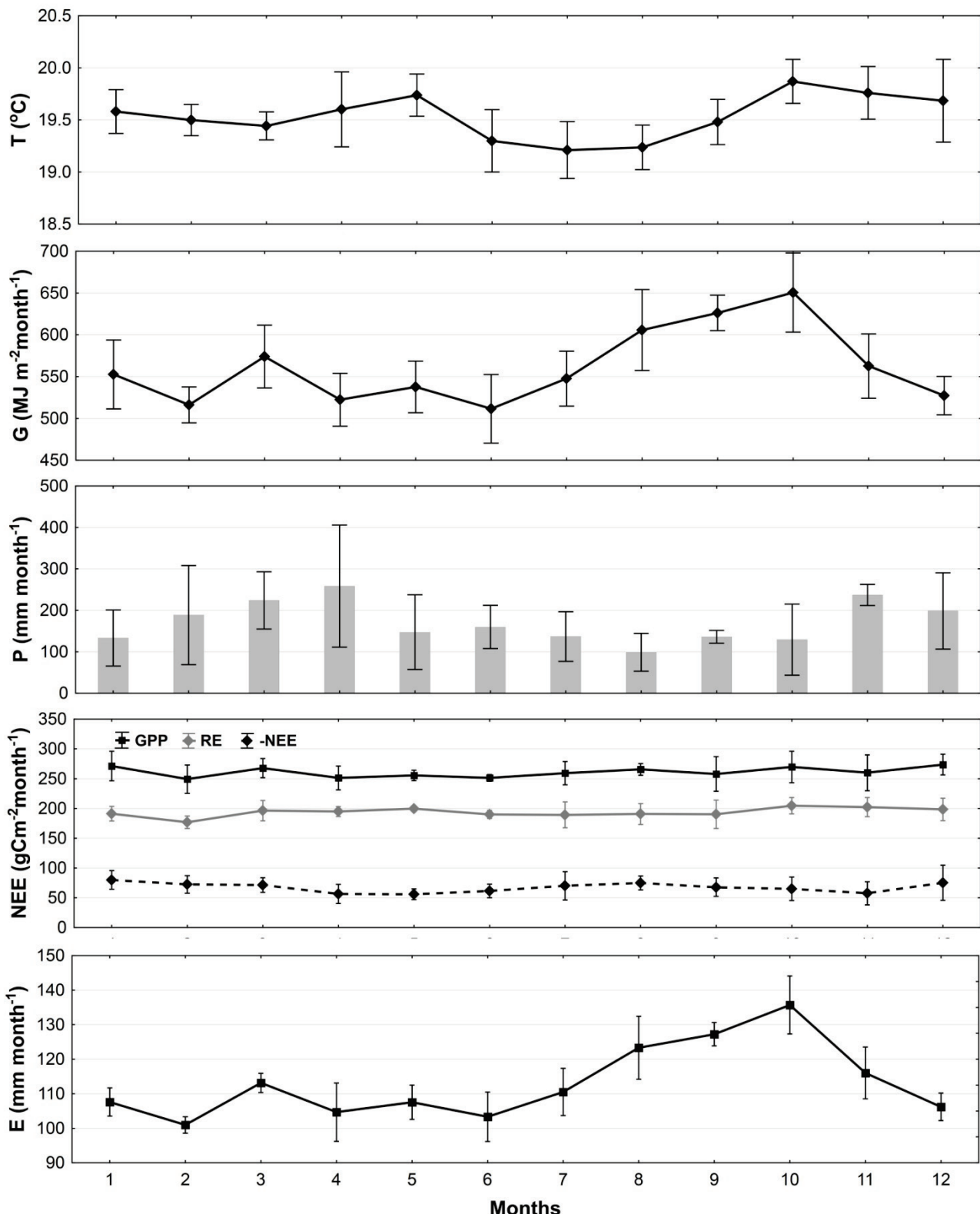


3  
4

5 Figure 1. Geographical location of a study area (marked by black triangle) in tropical rain forest in  
6 Central Sulawesi (Indonesia) and Nino4 and Nino3.4 regions.

7

1



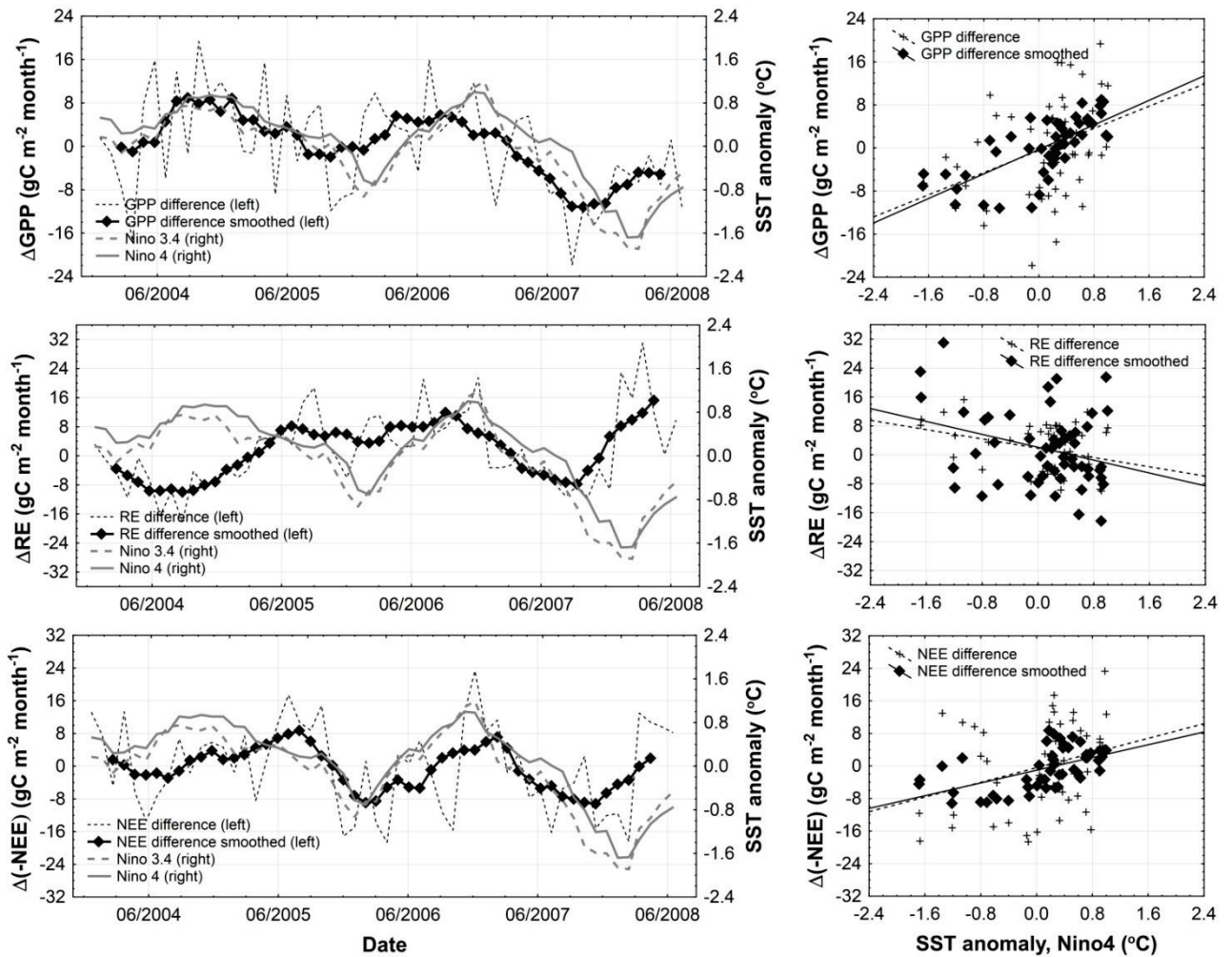
2

3

4 Figure 2. Mean intra-annual courses of air temperature ( $T$ ), global solar radiation ( $G$ ), precipitation  
 5 (P), NEE, GPP, RE and ET for the tropical rain forest in Bariri. Vertical whiskers indicate standard  
 deviations (SD).

6

1



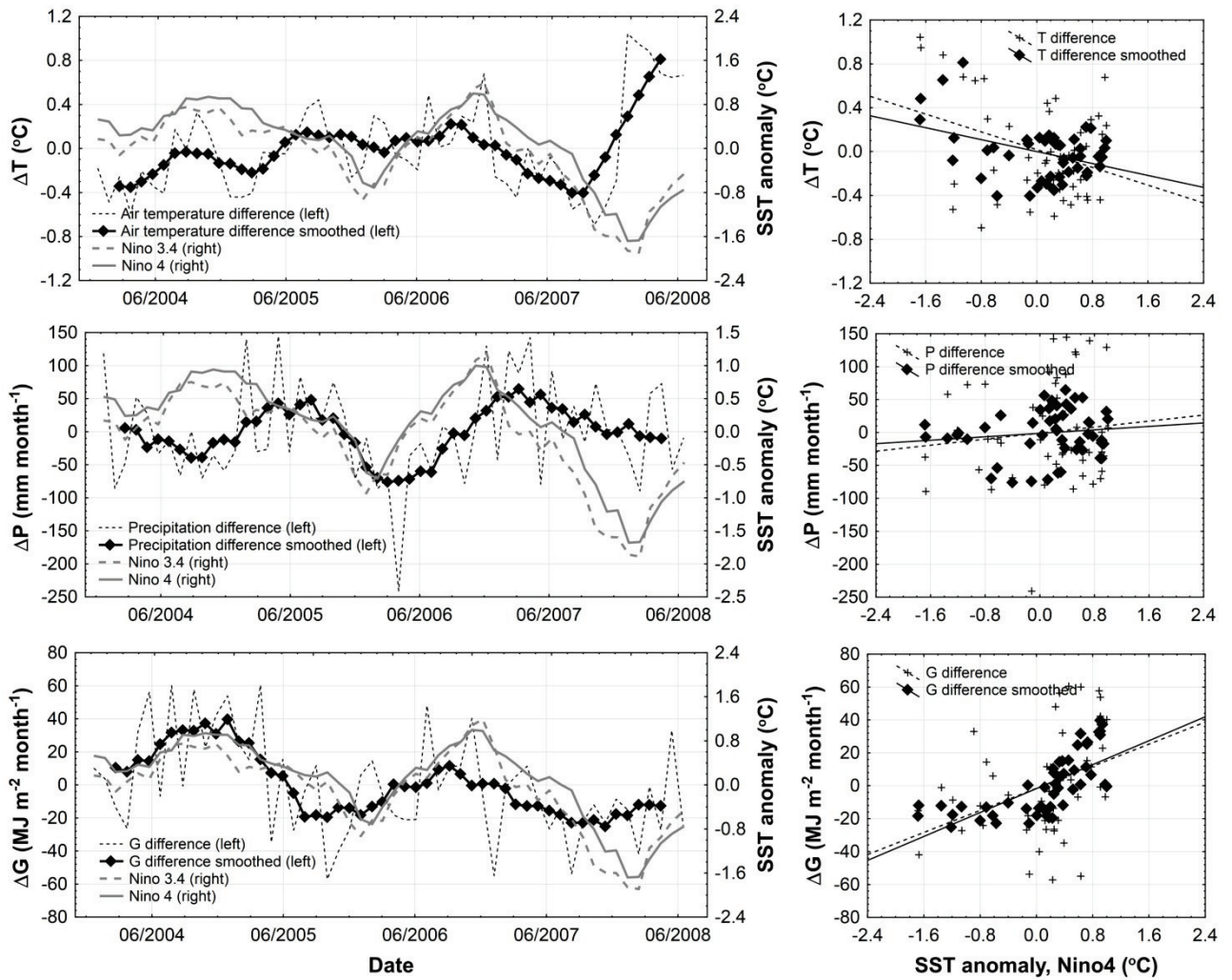
2

3 Figure 3. Comparisons of inter-annual pattern of SST anomalies in Nino4 and Nino3.4 zones of  
4 equatorial Pacific with variability of both deviations and 7 month ( $\pm 3$  months) moving average  
5 deviations of monthly GPP, RE and NEE values from mean monthly values of GPP, RE and NEE  
6 averaged over the entire measuring period from 2004 to 2008.

7

8

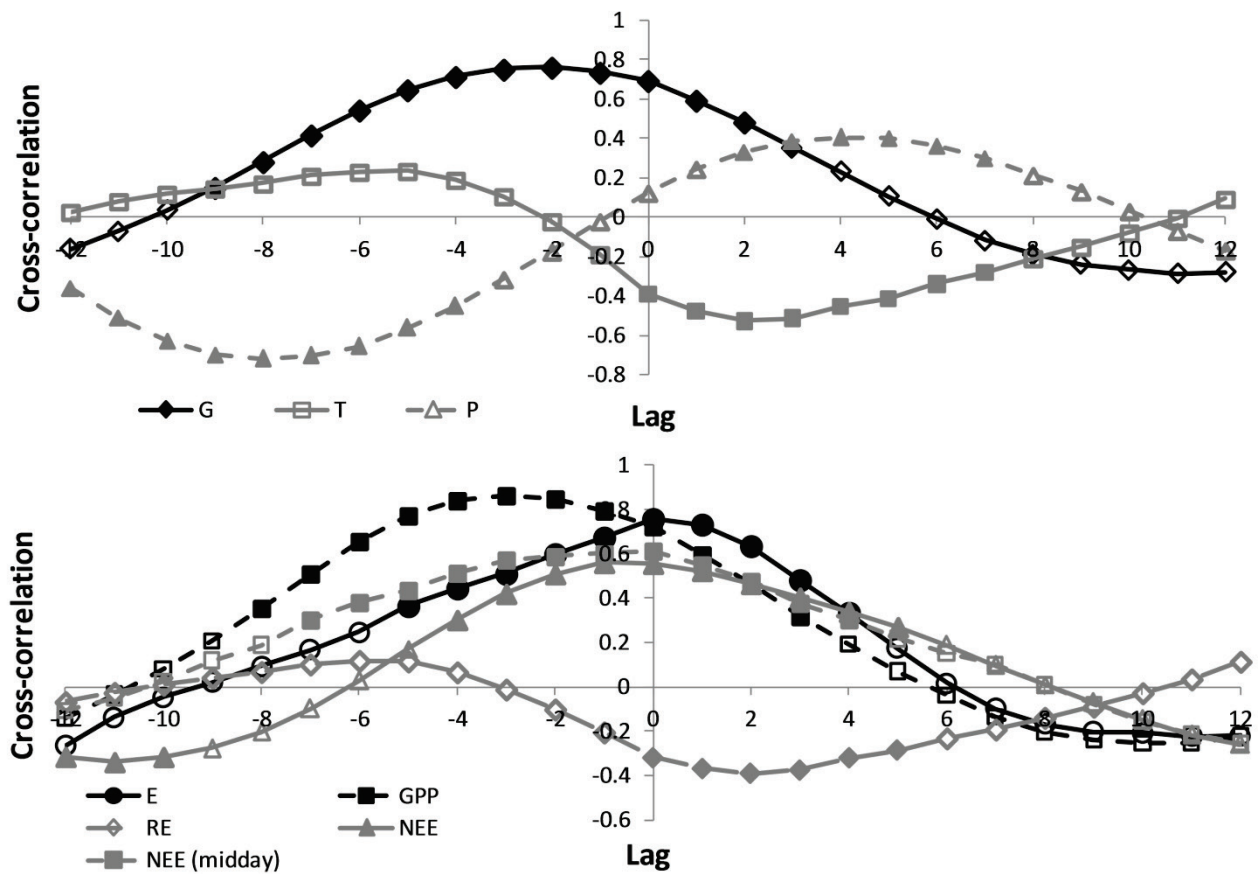
1



2

3 Figure 4. Comparisons of inter-annual pattern of SST anomalies in Nino4 and Nino3.4 zones of  
4 equatorial Pacific with variability of both deviations and 7 month ( $\pm 3$  months) moving average  
5 deviations of monthly air temperature (T), precipitation (P) and global radiation (G) values from  
6 mean monthly values of T, P and G averaged over the entire measuring period from 2004 to 2008.

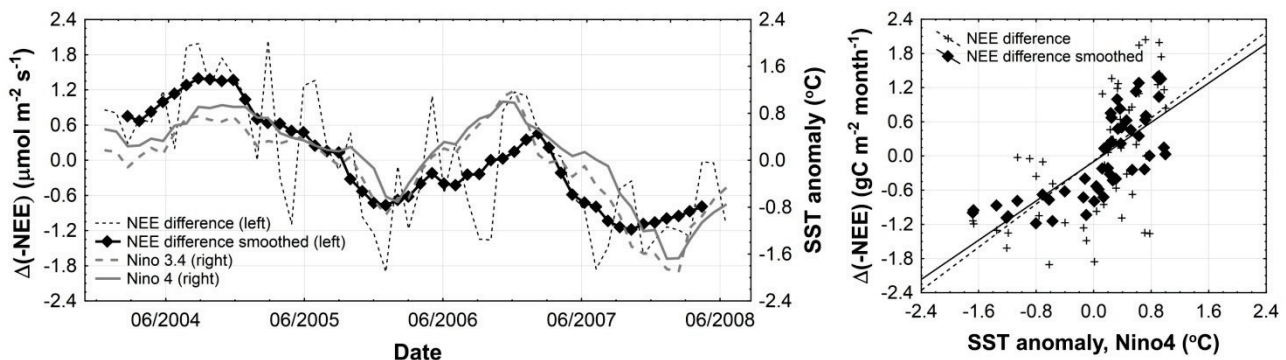
7



1  
2  
3  
4  
5  
6  
7  
8

Figure 5. Cross-correlation functions between  $\Delta G_{MA}$ ,  $\Delta T_{MA}$ ,  $\Delta P_{MA}$ ,  $\Delta E_{MA}$ ,  $\Delta GPP_{MA}$ ,  $\Delta RE_{MA}$ ,  $\Delta NEE_{MA}$  and midday  $\Delta NEE_{MA}$  values and SST anomalies in Nino4 zone of equatorial Pacific. Filled symbols are corresponded to  $p$ -value  $<0.05$  and non-filled symbols - to  $p>0.05$ . Lag step is 1 month.

1

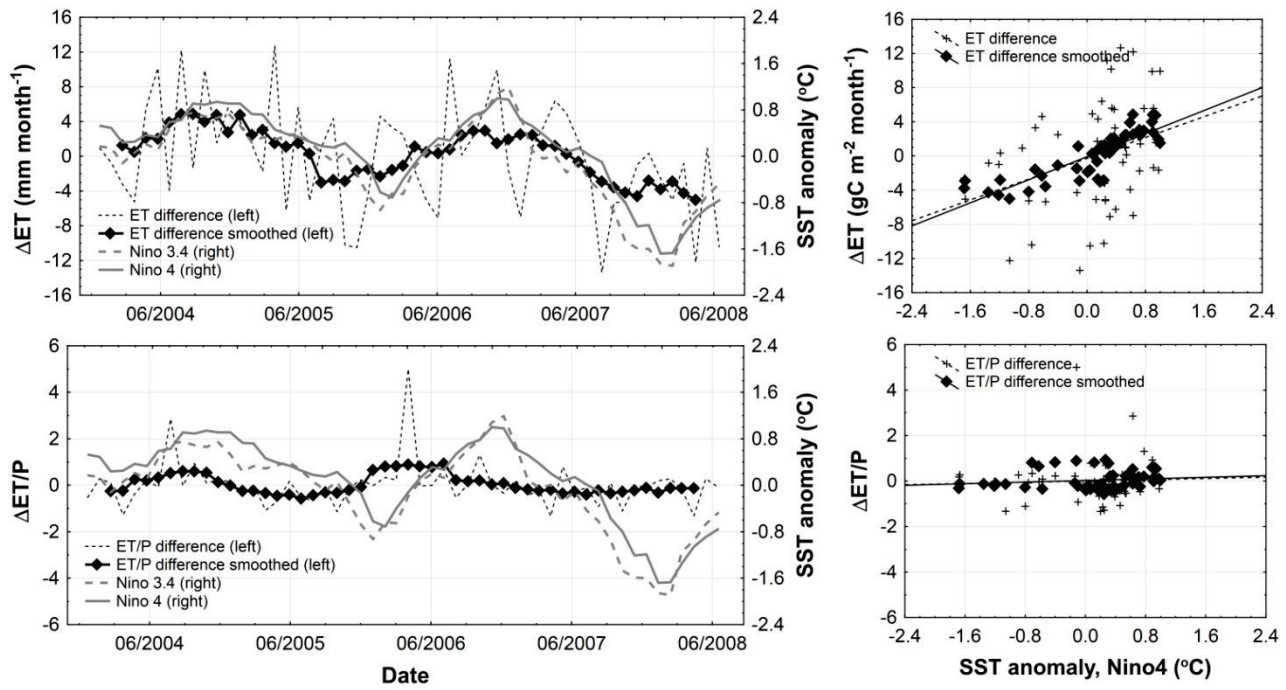


2

3 Figure 6. Comparisons of inter-annual pattern of SST anomalies in Nino4 and Nino3.4 zones of  
 4 equatorial Pacific with variability of both deviations and 7 month ( $\pm 3$  months) moving average  
 5 deviations of midday NEE (10:00-14:00) values from mean monthly midday values of NEE  
 6 averaged over the entire measuring period from 2004 to 2008.

7

1



2

3

4 Figure 7. Comparisons of inter-annual pattern of SST anomalies in Nino4 and Nino3.4 zones of  
 5 equatorial Pacific with variability of both deviations and 7 month ( $\pm 3$  months) moving average  
 6 deviations of monthly ET rate and ratio ET/P from mean monthly ET rate and ET/P averaged over  
 7 the entire measuring period from 2004 to 2008.

8

9